# Assessing the predictive ability of multispectral and geomorphometric data for soil rock fraction and bulk density

by

Nathan Brownstein

B.S., Millsaps College, 2019

A THESIS

submitted in partial fulfillment of the requirements for the degree

MASTER OF ARTS

Department of Geography and Geospatial Sciences
College of Arts and Sciences

KANSAS STATE UNIVERSITY
Manhattan, Kansas

2023

Approved by:
Major Professor
Arnaud J.A.M. Temme

# Copyright

# Abstract

In recent decades, significant progress has been made in digital soil mapping methods. However, gaps remain, particularly with respect to the quality of maps for sloped and stony land. Attempts to increase agricultural production on such land, for instance through robotic planters, require the development of higher resolution soil maps emphasizing properties like bulk density and stoniness that determine planter energy use. I test our current ability to predict these properties by relating them to widely available multispectral and geomorphometric data. Three study areas in Colorado, Minnesota and Missouri were selected to cover a range of climate and landscape settings. About 50 sample locations for each site were selected using a Latin hypercube of representative curvature and topographic wetness index to set sampling locations. Unusually large sample volumes were used in triplicate at each sample location to reduce negative bias in stoniness measurements. A series of commonly used geomorphometric variables, along with multispectral data, were then employed in regression models to assess predictive ability for bulk density and rock fraction. Results indicate the models for stoniness were incapable of establishing a relationship between it and the model variables in both Minnesota and Missouri. In Colorado, however, a moderate r-square of 0.52 was observed, suggesting some relationship may be identified. With respect to the bulk density, all three models reported weak r-squares, though the Colorado model performed the best. Possible explanations for this performance include the low variation in stoniness at the Colorado study area, the limited relief therein, or a lack of obstructive vegetation. However, additional research, such as the inclusion of multispectral indices, is likely necessary.

# Table of Contents

# List of Figures

# List of Tables

# Chapter 1 - Introduction

Though global food demand is increasing, yield growth appears to be lagging behind (Alexandratos and Bruinsma 2012, Ray et al. 2012). To meet anticipated demand in 2050, agricultural expansion on an additional 70 million hectares of usable land could prove necessary (Alexandratos and Bruinsma 2012). One means of expanding agricultural land involves employing self-propelled robotic planters on hillslopes too steep for traditional farming methods. These robots are smaller and lighter, reducing the risks of the vehicle toppling, and in turn allowing for employment on terrain inaccessible to traditional agricultural methods (Foley et al. 2011, Badgujar et al. 2022a, Badgujar et al. 2022b).

The differences between robotic planters and conventional tractors mean that different soil properties become important for productivity. Because of their limited power and energy, robotic planters are especially sensitive to changes in bulk density, while stoniness is generally undesirable in agricultural contexts. Therefore, the successful employment of robotic planters necessitates high resolution maps of these properties. However, the traditional focus on mapping productive arable land has led to a lack of interest in mapping less productive land, such as hillslopes which complicates the implementation of agricultural robotics. As a result, soils on steep or stony land are often mapped at lower levels of detail (USDA-NRCS Soil Science Division Staff 2017). Often, multiple soil types are mapped as associations within the same polygon, rather than as separate units. In such cases, it may be known and described which soil type is where in the landscape, but that knowledge has not been used to create finer-resolution polygons. Large polygons describing soil complexes or association with a large number of component soils cannot capture variations in properties at the scale needed to implement robotic planters.

Digital soil mapping is a computer-based approach to generating soil maps. Though many techniques and models may be applied to create predictive soil maps, the outcome is usually one or more rasters with cell values referencing specific soil information (Lagacherie and McBratney 2006). Digital soil mapping has been used to create soil maps at many scales, from regional maps to global projects (Stoorvogel et al. 2017, Dobos et al. 2001). Because digital soil mapping is not reliant on tacit knowledge or in-depth field surveys, it presents a more accessible means of mapping soils. Predictive models in digital soil mapping are highly customizable, with a wide array of quantitative approaches available (see McBratney, et al. 2003 for more discussion). However, many questions that could be addressed through digital soil mapping remain unanswered. In particular, maps pertaining to soils on subprime land or with respect to certain soil properties, such as stoniness, are often of lower quality compared to mapping performed on subdued or less stony terrain (USDA-NRCS Soil Science Division Staff 2017). To better understand the soil-landscape dynamics of soils on sloped land, more attempts to model and predict their properties based on landscape traits are necessary.

Digital soil mapping necessitates large spatial datasets and there is currently a great need for additional pedon-scale or better soil data and explanatory variables to build such datasets. In fact, soil properties may have significant local variation, making pedon-scale data insufficient (McBratney and Pringle 1999, Lagacherie and McBratney 2006), and perhaps necessitating a means of capturing local variation. To aid in creating higher resolution maps, an extensive array of explanatory datasets can be used in digital soil mapping projects, including geomorphometric variables, such as slope, topographic wetness index, curvature, landscape orientation, roughness, and terrain ruggedness index. However, inclusion of multiscale geomorphometric variables is not routinely done, leaving a gap in the modelling process (Miller et al. 2015). They used an array of variables at different scales along with multispectral data and associated indices. Multi-scale variables included were slope, profile and plan curvature, aspect, northness and eastness, relative elevation, and topographic position index (Miller et al. 2015). Miller, et al. (2015) found the use of multiple-scale geomorphometric variables resulted in better predictions for all soil properties examined—organic carbon, silt content, bulk density, and topsoil thickness—but that topsoil thickness and organic carbon models experienced the greatest benefit over more conventional modelling because such variables lack relationships with variables included in the conventional models (Miller et al. 2015).

## Objective

In this thesis, I will test the viability of a method of creating high resolution predictions for soil stoniness and bulk density using new soil pedon datasets and a combination of geomorphometric variables and multispectral data, with linear regression. If demonstrated viable, this method would allow for the creation of predictions of soil bulk density and stoniness needed for implementation of robotic agriculture on slopes too steep for conventional methods.

## Background

Bulk density is a measure of the mass of a soil within a given volume (Campbell 1994, Erbach 1987). Bulk density, a metric for soil quality, relates to a wide array of additional physical and chemical properties (Dam et al. 2005, Chaudhari et al. 2013). High soil bulk density can negatively impact root growth (Popova et al. 2016, Logsdon and Karlen 2004), and requires more energy to plow. Therefore, it has significant agricultural and engineering importance, such as overall suitability for infrastructure development, drainage, and both the energy cost and effectiveness of tilling (Erbach 1987).

There are two primary methods to measure bulk density: direct and indirect (Al-Shammary et al. 2018, Campbell 1994). Of the direct methods, some of the most popular include the core method, the clod method, and excavation (Al-Shammary et al. 2018, Vanguelova et al. 2016). In the core method, which I used and will expand upon in the methods section, a metallic cylinder is forced into the ground. This has the tendency to overestimate bulk density because the soil may be compressed by the cylinder (Vanguelova et al. 2016, Blake and Hartge 1986). Furthermore, core methods are considered ineffective in stony soils (Blake and Hartge 1986, McLintock 1959, Wirth et al. 2004). This is because stones can prevent the cylinder from being pressed down.

The clod method involves weighing a ped in air and in a liquid (Blake and Hartge 1986). In the clod method, a clump of soil is waterproofed with an impermeable coating, and then submerged in water. The weight of the soil in water of a known temperature is compared to its weight when measured in air, then both values, in conjunction with a oven-dry soil mass measurement are used to determine soil bulk density without the need for a direct measure of soil volume (Blake and Hartge 1986). Because it relies on a single soil structural element, this method is not appropriate to measure bulk density in soils that are structureless or very stony.

The excavation method is another approach, whereby backfilling a dug pit with a known mass and volume of outside material is performed, then the oven-dried mass of the material in the pit can divided by its volume to determine bulk density (Blake 1965, Erbach 1987). Historically, heavy fuel oil, heavy syrup, sand, and water-filled balloons have been placed in the pit to determine the volume (Erbach 1987, Beckett 1928). If the starting volume or material density and mass are known, then determination of the volume of material placed in the pit can be calculated by subtracting the remaining mass or volume of the sand or fluid from the starting mass (Blake 1965). The excavation method is preferred in cases where soil stoniness is high, but remains susceptible to inaccuracies on hillslopes and other nonlevel terrain (Bauer et al. 2014, Al-Shammary et al. 2018, Vanguelova et al. 2016). Challenges with the backfilling process have been documented, such as its time-consuming nature and proneness to error if roots or stones are encountered within the excavated area, and measurement errors in the substance used to fill the pit contributing to error (Vanguelova et al. 2016, Vincent and Chadwick 1994, Blake 1965). More recently, photogrammetry has been suggested as a means of volume calculation (Bauer et al. 2014). Indirect methods to estimate bulk density often require specialized equipment, such as transducers, electrical or radiometric tools (Deans and Milne 1978) and are thus not suitable in a project seeking to develop an accessible methodology.

Stoniness pertains to the proportional amount of stones within a soil body. High stoniness, particularly of hard and low-porosity lithologies, is also generally undesirable because stony soils often have reduced water storage capabilities and are readily permeable, which may provide the conditions needed for nutrient leaching (Carrick et al. 2013). Direct measures, such as gravimetric techniques, can be used to determine stoniness (Reinhart 1961). However, the method used in many soil descriptions is visual estimation (Alexander 1981), which requires extensive field experience to perform well. Visual estimation, as the name suggests, involves a field researcher examining the soil and estimating the volumetric proportion of stones therein. Resources, such as in the Field Book for Describing and Sampling Soils (Schoeneberger et al. 2012) provide visual references to aid in the estimation of stones, roots, or other material using this method.

Other methods, such as electrical resistance, have also been used (Tetegan et al. 2012). Electrical resistance methods work on the basis that the coarse fraction of the soil will impact electrical transmission (Tetegan et al. 2012). Electrical resistivity is often measured through 4 electrodes—two that current runs through, and two that detect the current, where the potential difference between the detecting electrodes is used to make determinations about electrical resistance in the soil body (Samouëlian et al. 2005). Tetegan, et al. (2012) tested the viability of field-scale resistivity measurements for soil stone content and compared them to visual estimation. They found that electrical resistivity is comparable to field estimation by a professional, with a difference of approximately 10% in certain locations (Tetegan et al. 2012).

## Soil Mapping

Modern soil science is underpinned by the soil-landscape paradigm, a conceptualization of soil based on five key tenets. First, individual soil-landscapes are characterized by similar soil. Second, that differences in the topography between two soil-landscapes beget visible distinctions between their soil bodies. Third, similarities in soil-landscapes result in similarities in their soils. Fourth, that soil-landscape units maintain recognizable relationships through space, and, finally, that predictions may be made about soil bodies once the soil-landscape dynamics in an area are understood (Hudson 1992).

Soil itself influences landscape development (Minasny et al. 2015). Historically, such relationships were understood and described through traditional soil mapping. Traditional soil mapping is, in many respects, similar to that of traditional field research in other fields. Soil scientists would survey the landscape, identifying and delineating soils as they went. This process leans heavily on personal estimation and is largely empirical (Carré et al. 2007). Furthermore, traditional soil mapping is rooted in tacit knowledge, which takes significant time to acquire (Hudson 1992).With the rise of digital soil mapping techniques, a new avenue of purely quantitative soil study was opened—digital soil mapping.

## Digital Soil Mapping Methods

### Interpolation and geographic methods

Digital soil mapping encompasses a wide array of statistical methods, each with varying data input requirements and outputs based on context. Digital soil mapping techniques often incorporate data into geographic or geostatistical models to develop predictions about soil properties in a given area (McBratney et al. 2003, Sanchez et al. 2009). These techniques have been used to create hundreds of regional, or even global soil maps (Stoorvogel et al. 2017, Mora-Vallejo et al. 2008), and are expected to replace traditionally prepared maps over the next decades.  Among the very earliest of these techniques, purely geographic models use only the spatial relationships between soils to make predictions about their properties. These approaches were used starting in the 1960s when spatially distributed, high-resolution data about variation in soil forming factors was still limited (McBratney et al. 2003). A variety of different interpolation methods have been used in the creation of these types of digital soil maps, including kriging, inverse distance weighting (IDW), and splines. Because of the impact different interpolation procedures can have on a soil map, care should be taken when selecting one (Omran 2012). Kriging (Krige 1951), IDW and splines are all ‘exact interpolators’(Omran 2012), meaning these techniques provide predictions that exactly equal observations in observed locations (Lam 1983). While splines and IDW may both be exact interpolation techniques, they generate predictions within different parameters. IDW predictions will always fall within the minimum and maximum observed values. That is to say, if value x is the minimum value recorded on a map, and value y is the maximum, IDW will never assign a value below x, or above y, to any location. With splines, however, values above recorded minimum and maximum are possible (Omran 2012).

Kriging, which bears the namesake of its creator, D.G. Krige (Krige 1976, Lam 1983, Krige 1951), was first used for mine value estimations (Krige 1976). There are two types of kriging worth mentioning here: universal and ordinary. Ordinary kriging is the methodology first developed by D.G. Krige (Cressie 1990), while universal kriging is a modification of that method by G. Matheron in 1971 (as cited in Lam 1983) for data with relationships that vary across space (Lam 1983). Kriging, according to Lam (1983: 132) “regards the statistical surface to be interpolated as a regionalized variable that has a certain degree of continuity”. Kriging is therefore predicated on the presence of spatial autocorrelation—nonrandom spatial patterns (Lam 1983). Ordinary kriging, employed in cases of stationarity, uses covariograms to aid in the understanding of autocovariance matrices in the data (Lam 1983). Covariance and distance have a theoretically inverse relationship—covariance will decrease the further distance is (Lam 1983). In reality, this relationship is more complex.

In cases where stationarity is not found, variograms are used instead (Lam 1983). Variograms “[represent] the relationship between the mean-square difference between sample values and their intervening distance” Lam (1983: 132). Variograms and semivariograms are generalized in the expression given by Lam (1983):

$$r = \frac{1}{2}N \sum_{i=1}^{N} [z(x_i + d) - z(x_i)]^2$$

Kriging’s strengths lie in its capacity for regionalization, though challenges with managing and calculating the drifts, neighborhood, and variogram can complicate this approach (Lam 1983).

## Environmental Correlation

In contrast to the pure interpolation methods discussed above, environmental correlation is a process by which select statistical analysis methods (Minasny et al. 2009) are employed to correlate soil properties with other environmental features and processes, with the ultimate goal of making predictions about these properties (McKenzie and Austin 1993**.** Minasny, et al. (2009) asserts generalized linear regression, tree-based techniques, and Bayesian approaches are well-suited for this purpose. Linear regression and decision trees warrant additional discussion.

### Linear Regression

Originally developed and published in the early 1970s (Nelder and Wedderburn 1972), linear regression allows for the statistical assessment of linear relationships. In its most basic presentation, linear regression utilizes some form of the function I = α + βE + ε (Sykes 1993 ,p.6). The components of this function are the y-intercept (α), the slope or coefficient of the line (β), and noise (ε). In Sykes’ example, I and E represent specific variables being measured, however I and E can also be thought of as generalized response and explanatory variables, respectively. Linear regression can be valuable when employed in situations with limited complexity, are fairly accessible, and can be interpreted with relative ease (Lane 2002). However, many other linear regression techniques see application in soil science, such as ordinary least squares (Eldeiry and Garcia 2008) and multiple linear regression (Lesch et al. 1995, Forkuor et al. 2017).

Regression can be classified broadly into one of two categories: simple regression, which is modelled with only one independent variable, and multiple regression, which is performed with more than one (Sykes 1993). Performing simple linear regression is straightforward, but complexity increases when multiple explanatory variables are used to model the same response variable (Sykes 1993). Multiple regression allows for the examination of how multiple independent variables serve to explain the response. Because in many cases multiple factors affect a single response, multiple regression can be superior to simple regression. In multiple regression, the expected equation resembles (Sykes 1993, p.8):

$$I = \alpha + \beta E + \gamma X + \varepsilon$$

Most of the constituents of this equation are the same as in the simple regression equation, save for the addition of X and γ. γ is another coefficient, while X is another explanatory variable (Sykes 1993). Though these types of functions can serve as powerful tools, they are not without their flaws. In spatial applications, linear regression struggles to cope with non-stationary relationships (Brunsdon et al. 1998).

## Decision Trees

Decision trees have been described as a “divide-and-conquer approach to [regression and classification]” (Myles, et al. 2004: p.18). Like with, generalized linear models (Lane 2002), decision trees produce easy to interpret results and are widely employed (Myles et al. 2004). The basis of decision tree methodologies is a matrix where *n* columns information are associated with each sample point (Myles et al. 2004). These columns, could, for example, hold field and laboratory collected soil information and geomorphometric variables for use in predictive soil mapping. The data is partitioned through the implementation of rules, then these partitions are statistically evaluated. Next the decision tree itself is assessed, followed by the elimination of rules determined to be superfluous (Myles et al. 2004). In soil science, decision trees have been used in a variety of applications, including disaggregation and digital soil mapping (Häring et al. 2012, Taghizadeh-Mehrjardi et al. 2014).

## Multispectral Data and Digital Elevation Models in Soil Mapping

As digital soil mapping continues to grow in popularity, so too does the importance of readily available, reliable, and useful data with which predictions can be made. This data can take many forms, from digital representations of elevation and derivatives thereof, to the spectral responses of the landscape. At its core, the data employed in soil mapping is largely contained within raster formats—where individual cells contain values corresponding to the metric being represented. Cells can contain values corresponding to a wide range of measurements, from elevation, slope, landscape curvature, landscape position, land use, and reflectance.

Multispectral data is a category of raster data comprised of multiple available spectral bands in raster format. Starting in the 1970s, satellite-borne multispectral sensors were launched (Lambin 2001), making a new form of remote sensing scientifically viable. Many remote sensing satellites have been launched since, with the LANDSAT series being counted among the most notable. Multispectral data has been used in land use, land cover change, public health, and many other applications (Hartfield et al. 2011, Xu and Gong 2007).

Digital elevation models (DEMs) are another source of information from which we can derive metrics to aid the understanding of soil properties. DEMs are rasters in which each cell holds a value denoting its elevation (Burrough and McDonnell 1998). Digital elevation models are often used to generate landscape metrics from the topographic information they provide (see Dobos, et al 2000 for an extensive accounting of this practice). Derived landscape metrics are often local, whereby each cell holds a value of the new derived dataset, such as with aspect, slope, and curvature (Temme et al. 2022). Common indices, such as topographic wetness index (TWI) (Sørensen et al. 2006, Beven and Kirkby 1979) and terrain ruggedness index (TRI) (Riley et al. 1999, Różycka et al. 2017) also provide values for each raster cell. Topographic wetness index is an index of upslope area and slope that provides information on the relationship between surface hydrology and topography (Sørensen et al. 2006). Sorenson states "[TWI] is defined as ln(a/tanβ) where a is the local upslope area draining through a certain point per unit contour length and tanβ is the local slope" (2006, p.101) TWI has seen extensive usage in the study of plant life, soil, and groundwater (Sørensen et al. 2006). Terrain ruggedness index is a metric for 'terrain heterogeneity', calculated as the sum elevation difference between a cell and all 8 neighbors (Riley et al. 1999).

The exclusive use of such continuous measures is not without complications, however. Temme, et al. (2022) note that landscapes can exhibit abrupt, discontiguous feature such as cliffs or ledges that may not be sufficiently captured with continuous landscape metrics. These abrupt changes in landscape may influence the properties of soils nearby them (Temme et al. 2022). Temme, et al. developed and tested 10 variables intended to capture discontiguous landscape features—namely ledges and cliffs—and their spatial relationships to each other and the terrain around them. The metrics they created are vertical and horizontal distance from higher and lower edges, dubbed VDHEDGE, HDHEDGE, VDLEDGE, HDLEDGE respectively. In cases where no ridges are present, two additional measures, dubbed HPOSEDGE and VPOSEDGE, contain fractional values indicating the relative relationship a location has to a higher and lower edge. Four more variables—HHCLIFF, HLCLIFF, SLHCLIFF, and SLLCLIFF—represent the elevation of the closest higher and lower cliff face from a location, and the slope changes approaching the top of the higher and bottom of the lower cliff (Temme et al. 2022). In addition to these new metrics, Temme, et al. (2022) used a suite of common landscape variables, such as slope, curvature, TWI, TRI, roughness, northness, eastness, insolation, vertical and horizontal distance to ridges and channels, and relative slope position. They found that model performance was enhanced by an average of 29%, as measured by the adjusted r-square values, with the inclusion of their developed metrics (Temme et al. 2022).

## Study Areas

Because agriculture occurs in many climate conditions and topographies, effort was made to examine the relationship soil stoniness and bulk density have to landscape under different conditions. Three study areas were selected to capture different climate, vegetation, and topographies within the United States. These sites are Pawnee National Grassland in Colorado, Finland State Forest, Minnesota, and Roaring River State Park in Missouri. One site, Pawnee Natl. Grassland, was chosen because it has little to no tall vegetation, allowing for better multispectral returns of the land surface, as opposed to treetops. Differences in the sites are reflected in their soils, too. Roaring River, MO, had a significantly higher average stone content than the other two sites, while Pawnee Natl. Grassland had the lowest stone content and highest average bulk density (Table 1).

**Table 1:** average bulk density and stoniness values based on collected sample data at ~5-8 cm depth.

| Site | Average Stoniness Pct. | Average Bulk Density |
|---|---|---|
| Roaring River (MO) | 32.3 | 0.59 |
| Pawnee Natl. Grassland (CO) | 1.31 | 1.01 |
| Finland State Forest (MN) | 13.6 | 0.52 |

**Table 2:** Average annual temperature, rainfall, elevation and study area size for the study sites from Prism (PRISM Climate Group at Oregon State University 2012) climate data and USGS 3DEP digital elevation models(US Geological Survey 2021-2022) .

| | Pawnee Natl. Grassland | Roaring River | Finland State Forest |
|---|---|---|---|
| Area ($km^2$) | ~800 | ~20 | ~1200 |
| Avg. Rainfall (mm) | 352 | 1169 | 796 |
| Temperature (C) | 9 | 14 | 3 |
| Avg. Elevation (m) | 1551 | 376 | 555 |

**Pawnee National Grassland** is a nearly 200,000 acre discontinuous United States Forest Service-managed grassland located in Northeastern Colorado, in Weld County (United States Forest Service). It is both the highest elevation and driest study area—at 1551m and with only an average of 352mm of precipitation per year (Table 2). During the quaternary, glacial episodes have led to dramatic changes in fluvial systems and overall geomorphology, such as proglacial lakes and altered stream flowpaths, the impacts of which can still be seen today (Wayne 1991). In areas that did not experience glacial coverage, eolian and fluvial deposits sourced from the Rocky Mountains acted as the primary sediment inputs, with the addition of deposits from proglacial lakes where applicable (Wayne 1991). The Colorado Piedmont section of the Great Plains physiographic region, where much of Pawnee National Grassland is located, is when compared to adjacent regions, of a lower average elevation (Wayne 1991). It has experienced erosion of all Miocene age stratigraphic units present elsewhere from fluvial action (Wayne 1991). Upper Cretaceous sedimentary rocks—namely claystones, siltstones, and shales—act as bedrock in a majority of the area. These softer rocks at the surface have resulted in a characteristic smooth surface (Wayne 1991). Quaternary deposition is mostly fluvial in origin, and associated fluvial features are commonplace (Wayne 1991). Cobble size and larger material, though prominent closer to the Rocky Mountains, is less pronounced as one moves further away from the range (Wayne 1991). Outside of the South Platte and Arkansas Rivers, a majority of remaining streams are small and seasonal (Wayne 1991).

Much of the privately held land interspersed between public tracts is rangeland. Semi-arid climate conditions prevail (Table 1). Pawnee National Grassland falls within the Great Plains physiographic province, a region dominated by the rain shadow of the Rocky Mountains (Wayne 1991). As a result of the distinct seasonal contrasts and limited rainfall, native vegetation is predominantly grasses (Wayne 1991), while topography ranges from flatlands to hills with gentle slopes. Soils tend towards sandier textures, with the dominant soil within the study area being Olney fine sandy loam, which constitutes about 31 percent of the study area, with other sandy or fine-sandy loams also comprising a significant portion (Figure 1). About 13 percent is mapped in complexes, mainly the Renohill-Shingle complex, which represents 12% of the study area (USDA NCRS Soil Survey Staff). Reported bulk density values range from 1.25 to 1.68 $g/cm^3$, based on a weighted average of all layers (USDA NCRS Soil Survey Staff).

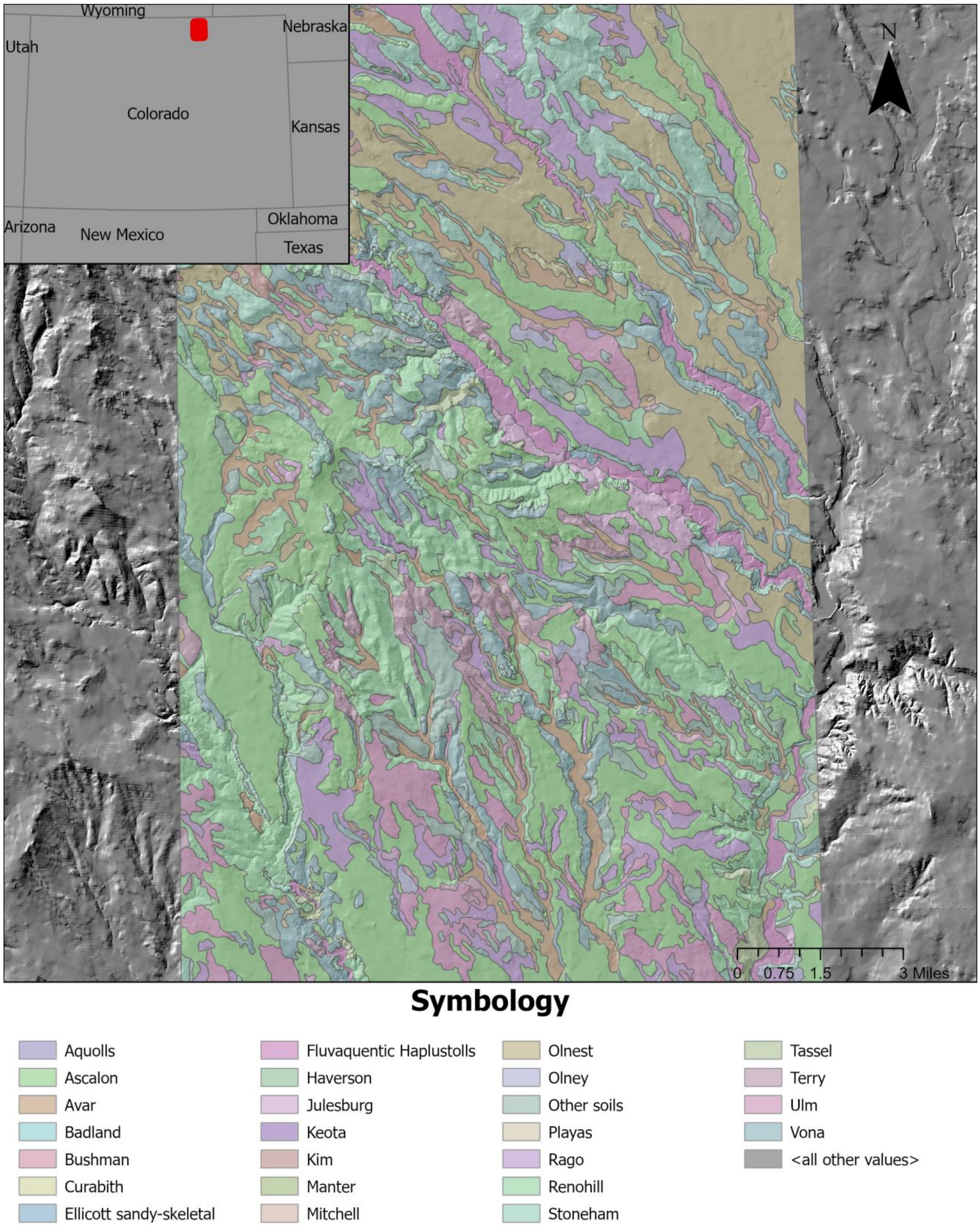


**Figure 1:** SSURGO Soil map units of the Colorado study area.

**Roaring River State Park** is a roughly 5,000 acre park in Southwestern Missouri, near the border with Arkansas and along a tract of the Mark Twain National Forest (Missouri Department of Natural Resources 2020). Mixed woodland vegetation and scree-lined steep hills present a topographic contrast to the two previous sites. The park features the highest average rainfall of the three study areas, along with significant relief (Table 2). The most pronounced soil series found within park bounds are the Reuter-Hailey Complex (found in 32.3 percent of the study area), a unit found in slopes ranging from approximately 35-60 percent and characterized as very or extremely gravelly throughout its horizons (USDA NCRS Soil Survey Staff). Other notable soil complexes are the Gatewood-Moko Complex, a stony unit found on 15-35 percent slopes, which accounts for around 15 percent of park area (USDA NCRS Soil Survey Staff). Reported weighted average bulk density values range from 1.21-1.47 g/cm$^3$.

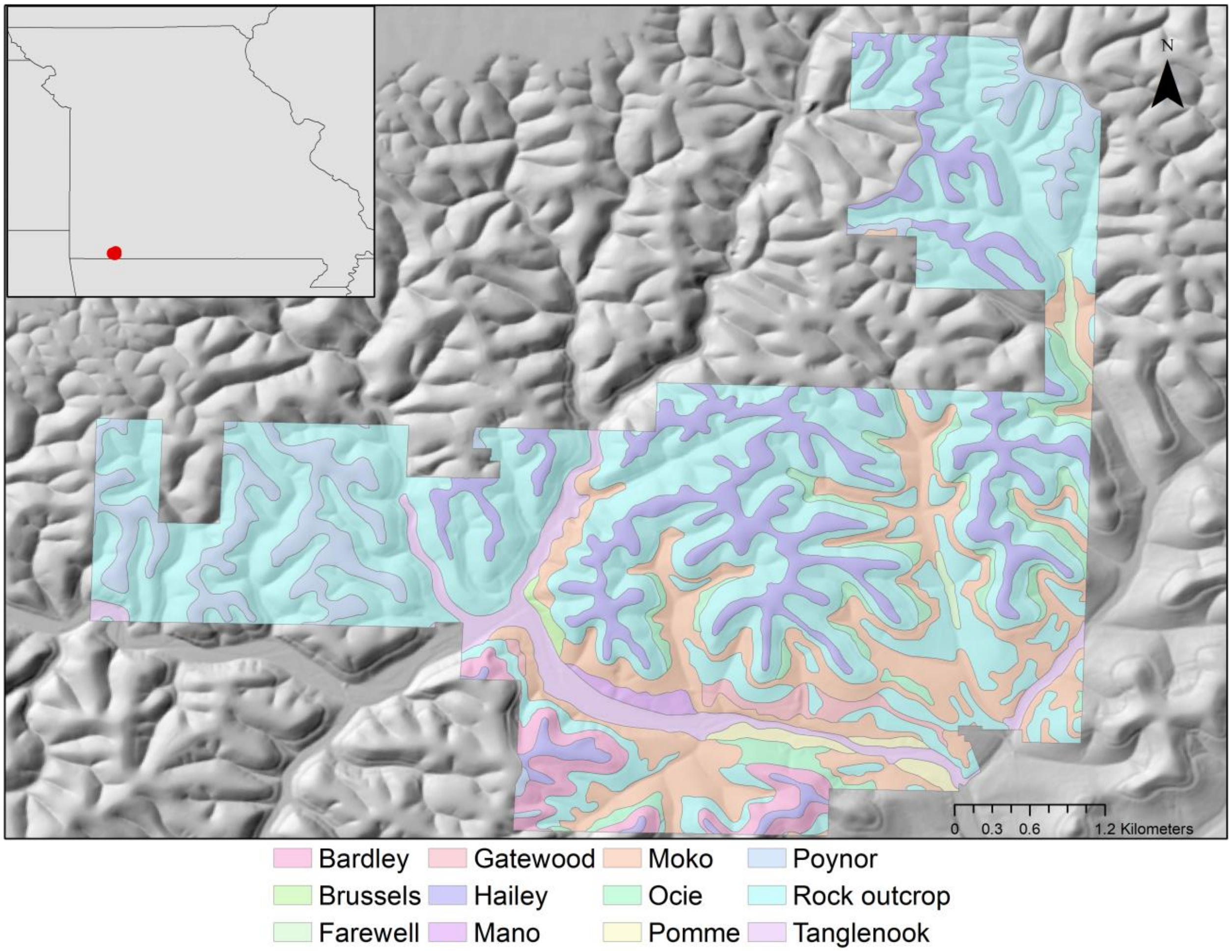


**Figure 2:** A soil-series level map of Roaring River State Park. Items shown are either soil series, complexes, or rock outcrops.

**Finland State Forest** comprises ~300,000 acres (Minnesota Department of Natural Resources 2003) bordering the southern boundary of the Superior National Forest. It is comprised largely of mixed or coniferous woodland vegetation, with topography ranging from flat land to gentle hills and ridges. The vast majority of the soil surrounding the study area has little or no soil information, per the gSSURGO data (USDA-NRCS Soil Survey Staff). Of the remaining mapped units, Rifle soils, an 'undifferentiated group' of soils, comprise the largest extent. Rifle soils are generally found on moraine depressions in woodland landcover.

During the Quaternary, much of Minnesota underwent significant glaciation, with the first episode occurring approximately 1.2 million BP (Minnesota Geological Survey 2017). This event would likely have included Finland State Forest. Sediments of glacial origin were predominantly deposited around 75 thousand years BP, corresponding to glaciation from the Laurentide Ice Sheet (Minnesota Geological Survey 2017). Following the Laurentide, several glacial lobes each deposited their own associated sediments. Three distinct Wisconsin age lobes created an intricate array of moraines and other glacial deposits (Minnesota Geological Survey 2017). In this context, the evidence of glacial deposits within the Minnesota study area are readily apparent. Glacial till and possible moraines were visible at the surface at several locations during field work. In lowland areas, peaty saturated soils were found, consistent with the simplified quaternary geologic map (Minnesota Geological Survey 2017).

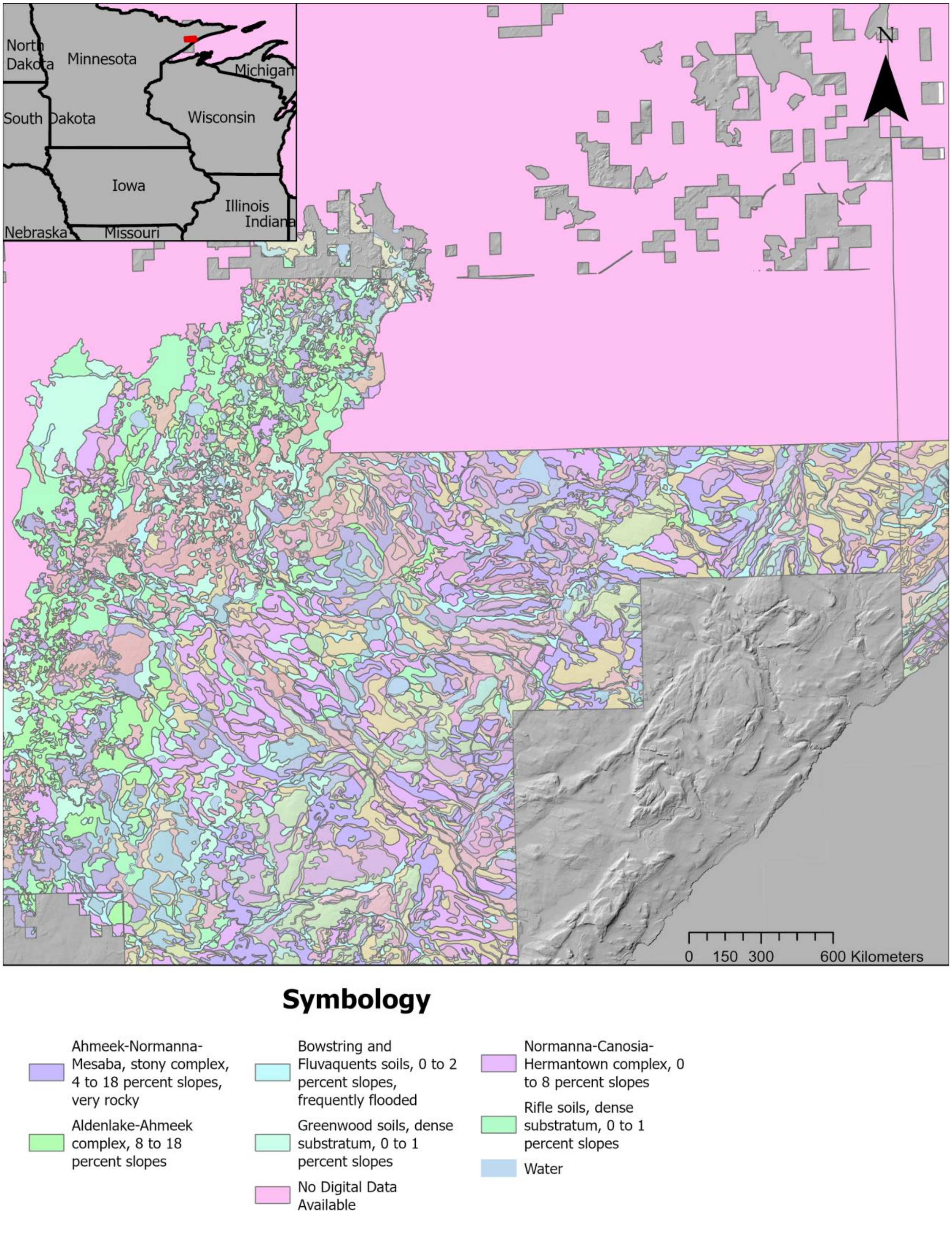


**Figure 3: A soil-series level map containing the Minnesota study area. Note that only the largest map units are shown in the legend.**

# Methods

The methods can be divided into three phases—a field phase, where a soil sampling scheme was created, and soil data collected, a laboratory phase where the soil data was analyzed, and a modelling phase, in which I explored whether stoniness and bulk density can be related to explanatory variables.

## Sampling design

A Latin Hypercube (Loh 1996, Viana 2016) based on representative curvature and terrain wetness index within the study area was used to determine sampling locations using the clhs, rgdal, and RSAGA packages (Roudier 2011, Brenning et al. 2018, Bivand et al. 2019). Values from the curvature and TWI rasters were extracted to a 100-meter buffer from roads derived from TIGER or county road and street data to generate sampling locations in Minnesota and Missouri. A 150 meter buffer from roads was used in the Colorado study site. At least 100 possible sample locations were generated at each location, with 200 generated in the Colorado study site. This allowed for skipping samples that were in inaccessible or unsafe areas. Ultimately, samples were collected from 59 locations in Finland State Forest, Minnesota, 50 locations in Roaring River State Park, Missouri, and 51 locations in Pawnee National Grassland, Colorado. Sample size was determined to balance time and cost constraints with statistical viability.

## Field sampling

After reaching each approximate sample location in the field, exact GPS coordinates were taken, and three soil rings were pressed into the ground within 3 meters of the centroid marked by the

GPS point - with the three sublocations selected randomly by blindly throwing a rock from the centroid. Soil rings with a volume of 272 $cm^3$ (height = 5.08cm) were pressed into the soil surface after vegetation and other organics were scraped away. In the very first set of samples collected from Minnesota, a larger 504.5 $cm^3$ (height = 8.128cm) makeshift PVC soil ring was used due to pandemic-related supply issues. If the soil rings were obstructed by rock fragments before being completely submerged, no soil sample was collected, and instead a visual estimate of soil stoniness to the nearest 5% was provided. In some cases, no soil samples could be collected from a site, reducing the number of available bulk density measurements for that study area. Additional features, such as the presence of large boulders, surface landscape features and presence of roots were also recorded. Observed dry, root-free sample masses ranged from 101.5-686.7 g for all study areas. The number of locations samples were collected from ranged between from 48-59, with a target of 50. Sampling was performed in triplicate at each location. In the Roaring River, Missouri study site, visual estimates were used in 63 cases of the 153 samples collected. In Colorado, no visual estimates were needed. In Minnesota, 31 of 166 samples analyzed were visual estimates of stoniness. Some samples in Minnesota were excluded from analysis because soil mineral horizon had not been reached due to extensive peat moss cover.

## Laboratory Methods

After collection, baking tins were weighed, and samples placed in them, before, in turn, being placed in a drying oven at 105°C for approximately 24 hours. The dried samples were weighed, then root and vegetative matter was manually removed before a second weighing to obtain the mass of roots and leaf litter.

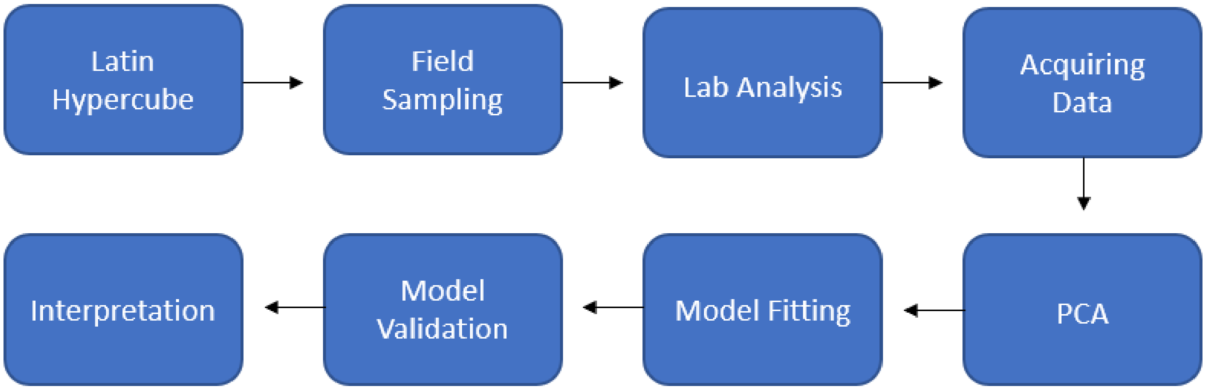


**Figure 4:** The methods used.

Afterwards, the entire dry samples were placed in a carbon oven at 450°C for 4 hours to burn off soil organic matter. To avoid incomplete combustion of my relatively large samples, I removed samples after 2 hours, then gently stirred to allow for more complete combustion of SOM instead of rotating the trays as Hoogsteen, et al. did (2015). After 4 hours, the samples were weighed to determine organic matter lost, then sieved with a 2 mm sieve. The resulting stone portion (>2mm) was separated and weighed, to calculate the soil stone fraction. Container mass was subsequently removed from the total mass to determine bulk density and stoniness. An estimated density of 2.6 g/cm$^3$ (Don et al. 2007) was used to convert the mass measure into a volumetric measure of stoniness, while 1 g/cm$^3$ was used for organic matter, based on Poeplau, et al.'s (2017) measure of root density. A bulk density formula from Poeplau, et al's (2017), was also used (their 'M2' formula, p.62) with some modifications. The original M2 bulk density formula is (Poeplau et al. 2017):

$$\text{SoilBD} = \frac{\text{mass}_{sample} - \text{mass}_{rock\ fragments}}{\text{volume}_{sample} - \dfrac{\text{mass}_{rock\ fragnments}}{\rho_{rock\ fragments}}}$$

To cope with samples containing very high amounts of organic matter—thereby causing extraordinarily low bulk density values—our bulk density calculation additionally removes the volume and mass of roots and other organics in addition to stone using a modified version of the above equation in the form of:

$$\text{SoilBD} = \frac{\text{mass}_{sample} - \text{mass}_{rock\ fragments} - \text{mass}_{organic\ matter}}{\text{volume}_{sample} - \frac{\text{mass}_{rock\ fragnments}}{\rho_{rock\ fragments}} - \frac{\text{mass}_{organic\ matter}}{\rho_{organic\ matter}}}$$

Mass of soil organic matter was considered to be the mass lost after four hours in a carbon oven at 450°C.

To assess whether 4 hours was long enough to remove all soil organic matter, a test batch of 4 samples was burned for a total of 8 hours, with mass recorded at 2-hour intervals to verify whether 4 hours of burn time was sufficient for my sample sizes. The results of this test demonstrate that nearly the entirety of the sample mass burning happens within the first 2-hour interval. Very little change was observed after a four-hour period, and therefore 4 hours was deemed sufficient


**Figure 5:** Cumulative percent organic matter removed over time in a carbon oven at 450C for 4 test samples.

## Data

A collection of 92 geomorphometric variables and multispectral satellite returns were generated or acquired for each study area. All variables were either derived from U.S. Geological Survey digital elevation models from the 3D elevation program (US Geological Survey 2021-2022). Geomorphometric variables were created from the DEMs at multiple scales to capture both small scale and larger scale topography, a strategy inspired by Miller, et al (2015). However, a much more comprehensive dataset was used in my attempt to assess the relationship variables have with stoniness and bulk density. Each of the 14 base geomorphometric variables were generated for 30, 50, 70, 110, 150, and 210-meter scales (Table 3). Eight bands (bands 1-7 and 10) of LANDSAT 9 Level 2 collection data (US Geological Survey 2019-2022) were used to provide multispectral info.

Table 3: the geomorphometric variables used in the model. Each was generated at multiple scales for a total of 84 geomorphometric variables.

| | | | | |
|---|---|---|---|---|
| Profile Curvature | Planform Curvature | Total Curvature | TWI | Roughness |
| Northness | Eastness | Slope | Vertical Distance from Channels | Horizontal Distance from Channels |
| Vertical Distance from Ridges | Horizontal Distance from Ridges | Relative Vertical Distance from Channels and Ridges | Relative Horizontal Distance from Channels and Ridges | |

## Modelling

Prior to the modelling phase, the data was extracted using the sp, sf and raster packages in R Studio (Pebsama 2018, Hijmans et al. 2020, Pebesma and Bivand 2005), then examined to identify relationships between explanatory variables, such as the geomorphometric data (Table 3), multispectral returns and the target variables of stoniness and bulk density. Both linear and several nonlinear relationships were examined. The linear relationship was concluded to be the strongest. Because of the high number of explanatory variables—8 multispectral bands and 84 geomorphometric variables—there was a need to reduce the number of variables to minimize overfitting. A suite of principal components were created from the geomorphometric variables and the multispectral data using the pls package (Hovde Liland et al. 2021). The top principal components representing >95% of all variation in the dataset were selected for inclusion into the model. The model principal components were then interpreted to glean insight into the variables they were comprised of, and their correlation to stoniness or bulk density. Those with correlation >+/-0.2 to their respective target variable of either stoniness or bulk density were examined thoroughly to associate them with specific landscape characteristics and positions, when possible. Principal components were included in a regression model, built using the olsrr v.0.5.3, tidyverse, Metrics v.0.1.4, moments v.0.14, dplyr, pls v.2.8-0, and MASS packages (Venables and Ripley 2002, Hovde Liland et al. 2021, Hebbali 2020, Wickham et al. 2020, Wickham et al. 2019, Hammer and Frasco 2018, Komista and Novomestky 2015), that runs 5 k-folds, thereby generating 5 r-square values, which are then averaged along with RMSE and relative RMSE to determine model strength.

Six linear regression models—one for bulk density and one for stoniness for each of 3 sites—were used in R to test the association of these components with bulk density and stoniness. Components with a correlation stronger than +/-0.1 were kept for inclusion in each model. The StepAIC function from the MASS package in R (Venables and Ripley 2002) is used to reduce the model to strengthen adjusted R-squares. StepAIC, or stepwise Akaike information criterion, is an automated best-fit model selection method used in cases where many explanatory variables are present (Zhang 2016, Flack and Chang 1987). The end result are 6 models with the strongest possible r-square values for this technique, in which the PCs are explanatory variables and bulk density or stoniness are the response variables.

## Validation

To validate the model, a k-fold cross-validation with k= 5 was used. Cross validation involves creating testing (~25%) and training (~75%) subsets. These two—testing and training—datasets are tested against each other repeatedly within the parameters of a model (Refaeilzadeh et al. 2009). K-fold cross validation, a common cross validation strategy, divides the data into a number of 'folds', then iterates the training and validation process for each fold. Model results can then be averaged (Refaeilzadeh et al. 2009). An average of the 5 adjusted r-squares, root mean square errors, and coefficient of variation root mean square errors for the each of the stepAIC reduced models from the k-folds were recorded to gauge model efficacy.

Root mean square error (RMSE) is a ubiquitous method to assess model accuracy, with an expression of (Wang and Lu 2018, p. 2):

$$\mathrm{RMSE} = \sqrt{\frac{\sum_{n=1}^{n}(\hat{r}_n - r_n)^2}{N}}$$

In which $\hat{r}$ is a prediction, $r$ is the actual data, and n is the quantity of values. Calculation of relative root mean square error is done by division of RMSE by the observation values' mean, such that (Temme, et al. 2022, p. 7):

$$\mathrm{RRMSE(x)} = \frac{\sqrt{\frac{\sum \; (x_{i,obs} - \; x_{i,pred})^2}{n}}}{mean(x)}$$

R-squared, an equation used to quantify the amount of variance explained by a given model, has substantial limitations when used in conjunction with models containing a high number of variables. For every variable used in the r-squared calculation, a corresponding increase in r-square will be noted, rendering an alternative necessary (Miles 2005). Adjusted r-square, expressed as (Miles 2005, p. 1657):

$$\text{Adj.}\, R^2 = 1 - (1 - \; \mathrm{R}^2)\frac{N - 1}{N - k - 1}$$

Which resolves the issues faced with r-square by placing the r-squared function over the number of predictor variables ($k$), which mitigates r-square increase alongside predictor variable quantity increase (Miles 2005).

# Results

## Representativeness

To demonstrate that the samples selected were generally representative of each study area's overall topography, I compared total curvature and topographic wetness index for both the samples and the entire study areas using the ggplot2 package in R Studio (Wickham 2016) (Figures 6-8). While the sample curvature and TWI distributions are similar to their sitewide counterparts, there are differences between the distribution of sample curvature and TWI and the sitewide curvature and TWI distribution for all three sites. This difference is most pronounced at the high- or low-end curvature and TWI values. In Minnesota, several locations could not be reached due to waterlogged or swampy terrain. It is plausible that such locations would fall within the upper limits of sitewide TWI (Figure 7). The Minnesota study area was the largest, and although more samples were collected here than in Colorado or Missouri, it still suffers from limited sampling. The extreme ends of landscape variation, such as steep or very curved areas, may not be as well represented.

Pawnee Natl. Grassland, by contrast, is a subdued, flat, or gently sloping study area. The range of curvature values is limited. Several extreme TWI outliers are observed in CO samples, however (Figure 6). While almost the entirety of the CO study area—and our own samples—fall on the leftmost side of the graph, several high sample TWI values can be seen. It is possible these values are caused by their proximity to roadways, drainage ditches, or the impacts of agricultural activity. Because the extreme values shown could be related to anthropogenic activity, sampling from areas with visible artificial features was undesirable. Great care was taken to avoid sampling directly from these locations, but they may still heavily influence the 10-meter cell from which the sample was collected.

Roaring River, Missouri has the most rugged terrain of the study areas. Steep hillslopes and significant relief between ridges and lowlands exist throughout the park. However, because of an extensive network of hiking trails, accessing all but the steepest or highest locations was straightforward. This allowed for a good representation of the overall landscape in my samples. While there are some differences in the distribution of the samples relative to the study area, the vast majority of the variation found is still captured in the samples. Based on the results of this comparison, I am satisfied that the samples adequately represent the overall landscape at each of the study areas.

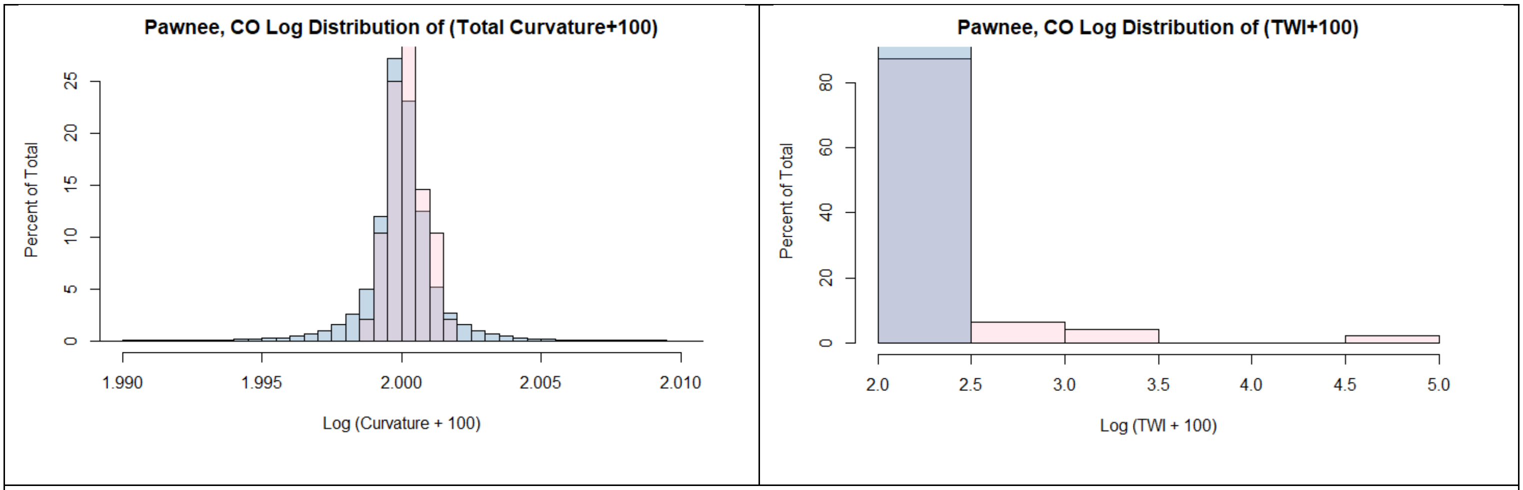


**Figure 6:** Comparison of the log distribution of sample curvature and sample TWI (pink) and the overall Colorado study area curvature and TWI (blue)

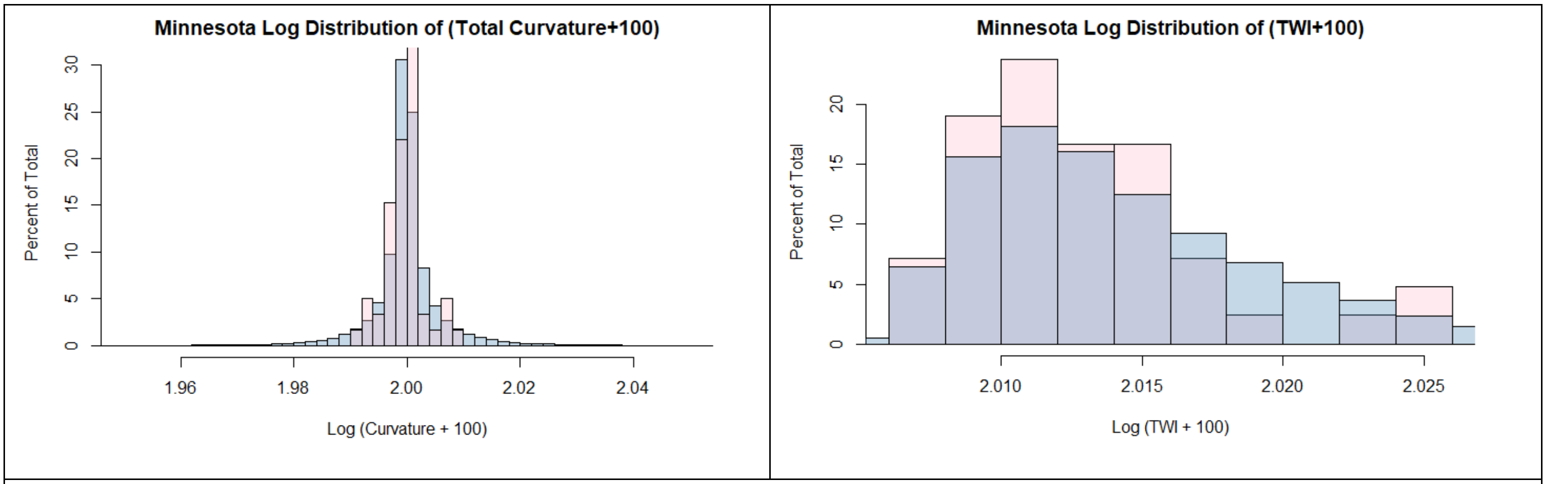


**Figure 7:** Comparison of the log distribution of sample curvature and sample TWI (pink) and the overall Minnesota study area curvature and TWI (blue)

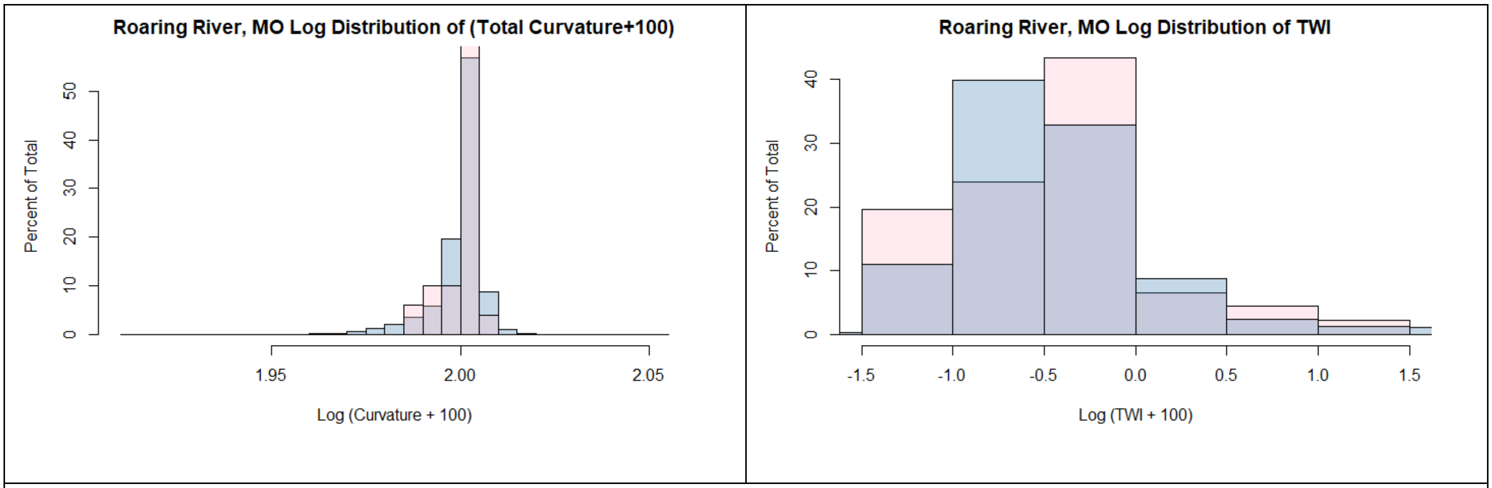


**Figure 8:** Comparison of the log distribution of sample curvature and sample TWI (pink) and the overall Missouri study area curvature and TWI (blue)

## Stoniness

A collection of descriptive statistics for each of the study areas highlights the differences in soil physical properties between them. The Missouri study areas has the highest variation in stoniness, with values ranging from near 1% to 44%, while Colorado has the least variation. Note that the maximum sampled stone values are in the mid-40% range. Higher stone contents required visual estimates because the soil ring could no longer be pressed. Visual estimates were included in the average stoniness reporting.

**Table 4:** Descriptive stoniness statistics for each study area.

| Site | Average and standard deviation of stoniness (%) | Min Sampled Stoniness (%) | Max Sampled Stoniness (%) | Max Est. Stoniness (%) |
|---|---|---|---|---|
| Colorado | 1.29 +- 0.64 | 0.00 | 14.11 | N/A |
| Minnesota | 13.62 +-7.75 | 0.00 | 46.20 | 100 |
| Missouri | 33.02+-10.98 | 0.92 | 43.99 | 100 |

The average stoniness values for each site ranged from 1.29-33.02%, with Colorado having the lowest average stone content and Missouri having the highest. Minimum values for all 3 sites were below 1% stone content, with Missouri having a minimum of 0.92% and the other 2 sites having samples with no stones. Maximum sampled values ranged from 14.11 for Colorado to 46.20 for Minnesota. In cases where a ring could not be pressed, the highest estimated stone values for both Missouri and Minnesota were 100% stone volume, indicating a very large rock was struck. The highest standard deviation was recorded for the Missouri study area, with +/-10.98%, while the lowest was found in Colorado, at +/-0.64%.

Principal components created from the suite of geomorphometric variables and multispectral data were then generated to incorporate into linear regression models. In the

Missouri study area, 12 principal components cover 95% of the variation of the original 93 variables. In Colorado, 14 components constituted 95% of variation. While in Minnesota, 19 principal components were needed to explain 95% of variation. The loadings of PCs with a correlation of greater than +/-0.2 to stoniness were examined to determine if they were associated with topographic characteristics (Tables 5-7).

Table 5: Colorado Stoniness PCs and proportion of variance.

| Component | Prop. Variance | Component | Prop. Variance |
|---|---|---|---|
| PC1 | 0.2849 | PC8 | 0.02436 |
| PC2 | 0.1619 | PC9 | 0.02208 |
| PC3 | 0.1409 | PC10 | 0.01851 |
| PC4 | 0.1031 | PC11 | 0.01446 |
| PC5 | 0.0718 | PC12 | 0.01115 |
| PC6 | 0.04712 | PC13 | 0.01005 |
| PC7 | 0.03208 | PC14 | 0.0079 |

Table 6: Minnesota Stoniness PCs and proportion of variance.

| Component | Prop. of Variance | Component | Prop. of Variance |
|---|---|---|---|
| PC1 | 0.2918 | PC11 | 0.01925 |
| PC2 | 0.1200 | PC12 | 0.01536 |
| PC3 | 0.1009 | PC13 | 0.01434 |
| PC4 | 0.08365 | PC14 | 0.01374 |
| PC5 | 0.05976 | PC15 | 0.0112 |
| PC6 | 0.05239 | PC16 | 0.00968 |
| PC7 | 0.04128 | PC17 | 0.00838 |
| PC8 | 0.03857 | PC18 | 0.00752 |
| PC9 | 0.03342 | PC19 | 0.0072 |
| PC10 | 0.02369 | | |

Table 7: Missouri Stoniness PCs and proportion of variance.

| Component | Prop. Of Variance | Component | Prop. of Variance |
|---|---|---|---|
| PC1 | 0.3583 | PC7 | 0.02625 |
| PC2 | 0.1775 | PC8 | 0.02553 |
| PC3 | 0.1476 | PC9 | 0.01913 |
| PC4 | 0.07199 | PC10 | 0.01663 |
| PC5 | 0.0531 | PC11 | 0.01116 |
| PC6 | 0.03757 | PC12 | 0.00584 |

For Colorado, 4 PCs met this criteria and 3 could be associated with specific landscape characteristics. PC1 has a moderate strength negative correlation to stoniness (-0.4) and is comprised of high TWI, high distance from channels, mid-low slope and roughness, and low distance from ridges. Thus, for Colorado, wet flat locations away from channels tended to have lower stone content. PC2 also contained high TWI loadings, mid-low roughness, low slope, lower distance from channels, and had a negative (-0.44) correlation to stoniness, meaning wet, flat areas near channels tended towards lower stoniness values. PC3 is comprised of high curvature, high northness and eastness, mid-high slope, roughness and low horizontal distance from channels. It was associated with lower stone content. PC9 could not be associated with a specific landscape characteristic based on its loadings.

For Minnesota, only a single loading bore a correlation of >+/-0.2. PC1. PC1 is negatively correlated with stoniness, and contains high loadings for relative vertical and horizontal distance, mid-low roughness, slope, total curvature and plan curvature, and low horizontal and vertical distance from channels. As such, it was determined to represent flat, near-channel areas. In the Missouri study area, 2 PCs—PC1 and PC3—were most strongly correlated with stoniness. PC1 loadings suggest locations with high distance from channels, mid-high northness, mid-low slope, and low distance from ridges may have higher stoniness, while PC3 comprises wet, flat areas or local depressions and has a negative correlation with stoniness.

**Table 8:** High correlation principal components in Colorado stoniness model.

| Component | Key Loadings | Topographic Association | Correlation |
|---|---|---|---|
| PC1 | High twi<br>High hdist from channels<br>Mid-High northness<br>Mid-High eastness<br>Mid-High vdist from channels<br>Mid-High prof curv (150m)<br>Mid-High spectral response<br>Mid-Low slope<br>Mid-Low roughness<br>Low vdist from ridges<br>Low hdist from ridges<br>Low rhdist<br>Low rvdist | Wet, flat areas away from channels | -0.40 |
| PC2 | High twi<br>Mid-Low hdist from channels<br>Mid-Low rougness<br>Mid-Low slope<br>Low vdist from channel | Wet areas near channels | -0.44 |
| PC3 | High eastness<br>High northness<br>High plan curv (30m)<br>High tcurv (30m)<br>Mid-High slope<br>Mid-High roughness<br>Mid-High plan curv (50,70,150,210m)<br>Mid-Low hdist from ridges<br>Mid-Low vdist from ridges<br>Low hdist from channels<br>Low prof curv (30m)<br>Low spectral response | Rugged, sloped, northeast-facing lands near channels | -0.31 |
| PC9 | High spectral (band 10)<br>High plan curv (50, 70, 110, 150m)<br>High prof curv (30, 50, 70m)<br>High tcurv (110m)<br>High twi (30m)<br>Mid-High eastness<br>Low hdist from ridges<br>Low hdist from channels | N/A | -0.25 |

**Table 9:** High correlation principal components in Minnesota stoniness model.

| Component | Key Loadings | Topographic Association | Correlation |
|---|---|---|---|
| PC1 | High rhdist<br>High rvdist<br>Mid-Low rougness (30m)<br>Mid-Low slope (30m)<br>Mid-Low tcurv (110, 150, 210m)<br>Mid-Low plan curv (70. 110, 150, 210m)<br>Low rougness (all other scales)<br>Low slope (all other scales)<br>Low hdist from channels<br>Low vdist from channels | Flat, near-channel areas | -0.20 |

**Table 10:** High correlation principal components in Missouri stoniness model.

| Component | Key Loadings | Topographic Association | Correlation |
|---|---|---|---|
| PC1 | High hdist from channels<br>High vdist from channels<br>Mid-High northness<br>Mid-High spectral (b1-b7)<br>Mid-Low slope<br>Mid-Low rougness<br>Low rhdist<br>Low rvdist<br>Low vdist from ridges<br>Low hdist from ridges | Relatively flat, north-facing locations near ridges | 0.24 |
| PC3 | High spectral<br>High twi<br>Mid-High prof (50)<br>Low slope<br>Low roughness | Wet, flat areas—local depressions | -0.27 |

## Stoniness Model Outcomes

Results of each model for stoniness, along with relative RMSE, are provided for comparison. Based on these outcomes, the regression models were most effective in Colorado, while poor performance is observed in Missouri and Minnesota. Root mean square error values demonstrate the Minnesota study area experienced the highest errors. Relative RMSE affirms the model for the Minnesota study area performed poorly relative to the model for the other two study areas. Intercepts and coefficients from each fold have been provided (Tables 12-14).

**Table 11:** The results of the reduced models for stoniness. RMSE values are in percent.

| Site | Adj. R-Squared | RMSE | RRMSE | N = |
|---|---|---|---|---|
| Colorado | 0.56 | 0.42 | 0.43 | 48 |
| Missouri | 0.05 | 0.34 | 0.25 | 49 |
| Minnesota | 0.02 | 1.91 | 0.60 | 59 |

Table 12: Colorado linear model intercepts and coefficient estimates.

| Component | Fold 1 | Fold 2 | Fold 3 | Fold 4 | Fold 5 |
|---|---|---|---|---|---|
| Intercept | 0.90874 | 0.96342 | 0.96008 | 0.93767 | 0.98598 |
| PC1 Coef. | -0.03821 | -0.05197 | -0.08182 | -0.05500 | -0.05835 |
| PC2 Coef. | -0.07494 | -0.07735 | -0.09127 | -0.08247 | -0.08710 |
| PC3 Coef. | -0.04476 | -0.06109 | -0.06302 | -0.05815 | -0.06447 |
| PC4 Coef. | 0.02333 | 0.03112 | 0.04720 | 0.03868 | 0.03049 |
| PC8 Coef. | 0.14174 | 0.10737 | 0.10928 | 0.07291 | 0.12556 |
| PC9 Coef. | -0.11542 | -0.12466 | -0.13541 | -0.14095 | -0.13960 |
| PC10 Coef. | 0.11639 | 0.07922 | 0.09873 | 0.05072 | 0.12267 |
| PC14 Coef. | 0.14618 | 0.12376 | 0.28254 | 0.07000 | 0.09427 |

Table 13: Minnesota linear model intercepts and coefficient estimates.

| Component | Fold 1 | Fold 2 | Fold 3 | Fold 4 | Fold 5 |
|---|---|---|---|---|---|
| Intercept | 3.3475 | 3.2839 | 2.8902 | 3.04726 | 3.3539 |
| PC1 Coef. | N/A | N/A | N/A | -0.07363 | N/A |
| PC4 Coef. | N/A | N/A | N/A | -0.11252 | N/A |
| PC6 Coef. | N/A | N/A | N/A | -0.10584 | N/A |
| PC7 Coef. | N/A | N/A | N/A | -0.12739 | N/A |
| PC9 Coef. | N/A | N/A | N/A | -0.22355 | N/A |
| PC11 Coef. | N/A | N/A | N/A | 0.40914 | N/A |
| PC12 Coef. | N/A | N/A | N/A | 0.27478 | N/A |

Table 14: Missouri linear model intercepts and coefficient estimates.

| Component | Fold 1 | Fold 2 | Fold 3 | Fold 4 | Fold 5 |
|---|---|---|---|---|---|
| Intercept | 1.415827 | 1.39122 | 1.407856 | 1.409521 | 1.40765 |
| PC1 Coef. | 0.013031 | N/A | 0.020353 | 0.009242 | N/A |
| PC3 Coef. | -0.026790 | N/A | -0.030977 | -0.023764 | N/A |
| PC4 Coef. | -0.022225 | N/A | -0.004882 | -0.021374 | N/A |

## Bulk Density

Based on the calculated bulk density values from Table 9, it can be observed that the sitewide average bulk density values for the Minnesota and Missouri study sites are lower than those reported for Colorado. This is likely due to the higher organic matter content of soil samples collected in these temperate environments in contrast to the sandier and less OM rich soil found in my Colorado study area. Because this SOM was burned off, less mass was present for final bulk density calculations at these sites.

**Table 15:** Bulk density average values and standard deviations by site.

| Site | Avg. Bulk Density ($g/cm^3$) | Min Bulk Density | Max Bulk Density |
|---|---|---|---|
| Colorado | 1.01+-0.07 | 0.64 | 1.39 |
| Minnesota | 0.52+-0.05 | 0.17 | 0.86 |
| Missouri | 0.59+-0.06 | 0.07 | 0.97 |

In the Missouri study area, 12 principal components explain 95% of variation. For Colorado, 14 components explain that variation. Nineteen PCs explain 95% of variation for the Minnesota study area. When possible, the loadings of components with a correlation of r-square >+/-0.2 to the target variable are examined and associated with topographic characteristics. PC1, PC3, and PC6 had the strongest correlations to bulk density for the Missouri study area. PC1, comprised of high distance from channels, mid-low slope and roughness, and low distance from ridges constitutes flat or gently sloped land around ridges and has a moderate negative correlation to bulk density. PC3 contains high loadings for roughness, slope, mid-high curvature, and low TWI, suggesting it represents steep, rugged, dry areas, and that these areas tend to have lower bulk density. PC6 could not be associated with a specific landscape characteristics. For

Minnesota, PC1 has a moderate negative correlation with with bulk density. Loadings of mid-high TWI, low distance from channels, low roughness and low slope mean it is likely associated with flat, wet areas near channels. Based on the loadings in PC5 and PC9 for Colorado, these components best fit gentle hills and locally wet depressions, respectively. In both cases, a positive association is found between these Colorado components and bulk density.

Table 16: Minnesota bulk density PCs and proportion of variance.

| Component | Prop. of Variance | Component | Prop. of Variance |
|---|---|---|---|
| PC1 | 0.2945 | PC11 | 0.01926 |
| PC2 | 0.1166 | PC12 | 0.0152 |
| PC3 | 0.09947 | PC13 | 0.01445 |
| PC4 | 0.08499 | PC14 | 0.01386 |
| PC5 | 0.05951 | PC15 | 0.01112 |
| PC6 | 0.05197 | PC16 | 0.0099 |
| PC7 | 0.04225 | PC17 | 0.00854 |
| PC8 | 0.03785 | PC18 | 0.00775 |
| PC9 | 0.0339 | PC19 | 0.00736 |
| PC10 | 0.02349 | | |

Table 17: Missouri bulk density PCs and proportion of variance.

| Component | Prop. of Variance | Component | Prop. of Variance |
|---|---|---|---|
| PC1 | 0.3396 | PC7 | 0.0288 |
| PC2 | 0.1870 | PC8 | 0.02739 |
| PC3 | 0.1322 | PC9 | 0.02106 |
| PC4 | 0.07866 | PC10 | 0.01637 |
| PC5 | 0.05967 | PC11 | 0.0124 |
| PC6 | 0.03891 | PC12 | 0.01028 |

**Table 18:** Missouri study area high correlation components in soil bulk density model.

| Component | Key Loadings | Topographic Association | Correlation |
|---|---|---|---|
| PC1 | High hdist from channels<br>High vdist from channels<br>Mid-Low slope<br>Mid-Low rougness<br>Low rhdist<br>Low hdist from ridges<br>Low vdist from ridges | Flat or gently sloped uplands near ridges | -0.41 |
| PC3 | High roughness<br>High slope<br>Mid-High plan curv (30, 50, 70m)<br>Mid-High tcurv (30, 50, 70m)<br>Low twi<br>Low eastness<br>Low spectral | Steeply sloped, rugged areas | -0.26 |
| PC6 | High northness<br>Mid-High rhdist<br>Mid-High hdist from ridges<br>Mid-Low plan curv (30m) | N/A | -0.27 |

**Table 19:** Minnesota study area high correlation components in soil bulk density model.

| Component | Key Loadings | Topographic Association | Correlation |
|---|---|---|---|
| PC1 | High rvdist<br>High rhdist<br>Mid-High vdist from ridges<br>Mid-High twi<br>Low vdist from channels<br>Low hdist from channels<br>Low rougness<br>Low slope | Wet, flat areas near channels | -0.39 |

**Table 20:** Colorado study area high correlation components in soil bulk density model.

| Component | Key Loadings | Topographic Association | Correlation |
|---|---|---|---|
| PC5 | High hdist from channels<br>High tcurv (70, 110m)<br>Low spectral (bands 1-7)<br>Low prof curv (30, 50, 70, 110m)<br>Low roughness (210m) | Gentle hills away from channels | 0.27 |
| PC9 | High spectral (band 10)<br>High twi (30m)<br>High plan curv (50, 110, 150, 210m)<br>High prof curv (30m)<br>Low northness<br>Low twi (210m)<br>Low eastness (30m) | Locally wet, regionally dry areas—depressions? | 0.37 |

## Bulk Density Model Outcomes

Results of each model for soil bulk density, along with RRMSE, are provided for comparison. Some sample locations have no ring press data in Minnesota and Missouri. Because no soil samples could be collected at that location, no measure of bulk density could be calculated (see Field Sampling in the methods). As such, there are fewer samples used in models from both the Minnesota and Missouri study area. Intercepts and coefficient estimates are also provided (Tables 22-24). Unlike with the stoniness models, the results of the bulk density models do not show a large disparity in model performance. Per relative RMSE, Colorado still performs the best, but model performance is not far behind in Minnesota and Missouri.

**Table 21:** Results of linear regressions of bulk density values with the models. Adjusted R-squared provided for reduced models.

| Site | Adj. R-Squared | RMSE | RRMSE | N = |
|---|---|---|---|---|
| Colorado | 0.21 | 0.11 | 0.11 | 48 |
| Missouri | 0.19 | 0.19 | 0.32 | 42 |
| Minnesota | 0.16 | 0.12 | 0.23 | 57 |

Table 22: Colorado bulk density model intercepts and coefficient estimates.

| Component | Fold 1 | Fold 2 | Fold 3 | Fold 4 | Fold 5 |
|---|---|---|---|---|---|
| Intercept | 1.01774 | 0.987716 | 1.0274928 | 0.994589 | 1.003775 |
| PC2 Coef. | N/A | 0.007097 | 0.0074659 | 0.008767 | 0.005813 |
| PC4 Coef. | N/A | 0.002206 | 0.0003607 | 0.006435 | 0.005808 |
| PC5 Coef. | N/A | 0.017999 | 0.0143507 | 0.021618 | 0.009910 |
| PC6 Coef. | N/A | -0.002753 | -0.0124668 | -0.018400 | -0.019038 |
| PC7 Coef. | N/A | -0.006300 | -0.0157297 | -0.027500 | -0.008980 |
| PC8 Coef. | N/A | 0.023929 | 0.0190613 | 0.007057 | 0.016236 |
| PC9 Coef. | N/A | 0.034611 | 0.0406245 | 0.031896 | 0.030629 |
| PC12 Coef. | N/A | -0.021029 | -0.0005848 | -0.021804 | -0.029290 |
| PC13 Coef. | N/A | -0.045153 | -0.0310695 | -0.023625 | -0.010524 |
| PC14 Coef. | N/A | -0.016180 | -0.0428490 | -0.027968 | -0.026869 |

Table 23: Minnesota bulk density model intercepts and coefficient estimates.

| Component | Fold 1 | Fold 2 | Fold 3 | Fold 4 | Fold 5 |
|---|---|---|---|---|---|
| Intercept | 0.51795 | 0.5404 | 0.512256 | 0.5271134 | 0.521454 |
| PC1 Coef. | N/A | N/A | -0.011494 | -0.0103229 | -0.010927 |
| PC2 Coef. | N/A | N/A | -0.004803 | -0.0063785 | -0.006997 |
| PC4 Coef. | N/A | N/A | -0.007054 | -0.0114758 | -0.013515 |
| PC8 Coef. | N/A | N/A | -0.009919 | -0.0009222 | -0.009319 |
| PC13 Coef. | N/A | N/A | -0.013035 | -0.0252148 | -0.008237 |
| PC14 Coef. | N/A | N/A | 0.020106 | 0.0112405 | 0.031073 |

Table 24: Missouri bulk density model intercepts and coefficient estimates.

| Component | Fold 1 | Fold 2 | Fold 3 | Fold 4 | Fold 5 |
|---|---|---|---|---|---|
| Intercept | 0.5799578 | 0.62263 | 0.583722 | 0.628397 | 6.628e-01 |
| PC1 Coef. | -0.0182314 | N/A | -0.017973 | -0.019026 | 1.206e-02 |
| PC3 Coef. | -0.0120188 | N/A | -0.023972 | -0.013118 | -2.213e-02 |
| PC4 Coef. | -0.0002291 | N/A | -0.016906 | -0.012506 | -2.766e-02 |
| PC9 Coef. | -0.0331822 | N/A | -0.007826 | -0.018151 | -9.597e-05 |
| PC11 Coef. | 0.0582623 | N/A | 0.048959 | 0.038204 | 3.325e-02 |
| PC12 Coef. | -0.0650416 | N/A | -0.016463 | -0.031145 | -3.127e-02 |

# Discussion

## Stoniness

The Colorado study area had 4 components with a correlation greater than +/-0.2—PC1, PC2, PC3, and PC9. PC1 had a correlation of -0.40 to stoniness and represents wet, flat areas away from channels. PC2 had a correlation of -0.44 and is associated with wet areas near channels. PC3 corresponds to more rugged, sloped, northeast facing areas and had a correlation of -0.31 to stoniness. PC9 could not be assigned to any specific landscape feature, and has a correlation of -0.25. In Minnesota, PC1 represents flat, near channel areas and has a -0.20 correlation to stoniness. While, for Missouri, PC1 and PC3 were the highest correlation components, with correlations of 0.24 and -0.27, respectively. PC1 is associated with relatively flat, north-facing locations near ridges, while PC3 is associated with wet, flat areas, and/or local depressions.

In Colorado, all three high correlation PCs were negatively associated with stoniness. Thus, wet flat areas away from channels, wet areas near channels, and more rugged, sloped land all tended to have lower stone content. Several factors may provide context for these results. The first is that the Colorado study area is significantly more subdued than the other two study areas. The difference between a more rugged landscape feature and a smooth one is more minor. The second is the low variation in stoniness found throughout the site. With an average stoniness 1.29 % +/- 0.64, stoniness is not highly variable even though it may trend lower in these locations. PC1 likely represents low energy environments away from sources of large stone contents, so high stone content is unlikely. PC2 is more difficult to explain. Channels in the Colorado study area were generally ephemeral. Perhaps these channels transport and deposit material overwhelmingly comprised of sand, and stones do not often enter the channel. In such a case, a negative correlation with stoniness would be observed. More rugged slopes exhibited no observable difference in stoniness during field work. The majority of the soil at the surface was sandy, with very few fragments exceeding 2mm. This stronger negative relationship to stoniness for both PC2 and PC3 cannot be readily understood through field observations.

In Minnesota, PC1, representing flat, near channel areas—such as wetlands—have a weak negative correlation to stoniness. Field experience corroborates wetlands in the study area generally exhibited lower stoniness. For the Missouri study area, relatively flat, north-facing locations near ridges (PC1) have a weak positive correlation with stoniness. Ridges in the study area tend to be comprised of chert or limestone. Weathering results in fragments breaking off and depositing on areas below the ridges. A tendency of higher stoniness in areas near these ridges is not unexpected. With respect to the wet, flat areas and depressions PC3 appears to represent, this too matches field observations. Wet lowlands were often less stony than drier uplands. Ridges in upland areas were the predominant source of high stone content, meaning these wet lowlands were often located away from large numbers of ridges, and thus, sources of stones.

## Stoniness Model Performance

Of the three study areas, the model was only able to provide viable results for Pawnee National Grassland, CO. In the Minnesota and Missouri study areas, poor R-square values suggest stoniness could not readily be explained by the model. The Colorado study site, however, with an adjusted r-square of 0.56, was promising. An examination of loadings in the most strongly correlation principal components for the Pawnee National Grassland stoniness model reveals all high correlation PCs have negative correlation with stoniness. That is to say, stoniness values tend to be lower in wetter areas and sloped land near channels. Given the

Colorado study area has the lowest topographic variation and the lowest average stone content and variation therein, the variations ‘explained’ by these components are slight.

With respect to the unsuccessful models for Roaring River State Park, MO, and Finland State Forest, MN, a number of speculative reasons for the model’s failure can be surmised. The regression model used was strictly linear. Though testing on alternative models, mainly a decision tree and nonlinear models, were performed on Roaring River, these tests did not demonstrate a better fit than a linear model. It is possible still that a different model would have generated more viable results. It is further possible StepAIC reduction was an inadequate choice for both models, and excluded variables too aggressively. Finally, it is possible the selection of predictor variables chosen, as extensive as it was, was simply insufficient at capturing the interrelationship between soil stoniness and the landscape. Principal component analysis trimming—used to reduce the number of variables included in the regression models further—may have also proved too strict. In both of these study areas, lithology may also play a confounding role. The Minnesota study area contains glacial till and other features associated with glaciation that may not be adequately represented by the geomorphometric variables. In the Missouri study area, chert ridges provide large quantities of scree to the areas below. Having a way to identify these locations and inform the model with lithology would provide an avenue for possible model improvement.

The highest correlation principal components in the Minnesota study area represents near channel, flat locations, but its low correlation to stoniness (-0.20) offers little predictive value. For the Missouri study site, two high correlation components were identified. PC1 appears to constitute relatively flat areas near ridges, and has a positive (0.24) association with stoniness.

PC3 may represent wet, flat depressions in the landscape, and has a negative correlation (-0.27) with stoniness. In both cases, these correlations are weak.

## Bulk Density

In the Colorado study area, the highest correlation components were PC5 and PC9, which are associated with hilly areas away from channels, and wet depressions, respectively. Both variables bore weak-moderate positive associations with bulk density—0.27 and 0.37 respectively. For Minnesota, only a single variable had a correlation with bulk density stronger than +/-0.2. This component, PC1, was associated with wet, flat areas near channels, and has a moderate negative correlation with bulk density. For Missouri, three components with negative correlations ranging from weak to moderate were identified. PC1, which constitutes flat or gently-sloping uplands had moderate negative correlation (-0.41) with bulk density, PC2, which comprises areas with steeply-sloped, rugged terrain near ridges, and PC6, which could not be identified with any specific landscape features.

PC5 and PC9 in the Colorado study area represent gentle hills away from channels and locally wet/regionally dry areas respectively. Both of these components are positively correlated to bulk density. Thus, bulk density trends higher in these locations. In the case of PC5, higher bulk density may be attributed to limited quantity of SOM and stones. Hillslopes in the study area have limited vegetative cover, and stones in the study area are found in limited quantities. As such, a high proportion of mineral content that remains after root removal and ignition is present in these samples. PC9 is more difficult to explain. On the one hand, regionally drier areas may be associated with lower vegetative content and SOM. However, it would appear that locations fitting PC9 may be wetter depressions, which might be more conducive to vegetative growth and the buildup of SOM, which would in turn lead to lower bulk density values. The moderate correlation PC9 has with bulk density cannot be readily explained based on the available information. In the Minnesota study area, PC1 has a negative correlation with bulk density. PC1 corresponds to wet, flat areas near channels. These locations likely have more SOM, which is both less dense than mineral matter and is removed in the carbon oven, resulting in lower bulk density values. In Missouri, PC1, PC2, and PC6 all negatively correlate to bulk density. PC1 and PC2 are both associated with uplands. PC1 represents flatlands, while PC2 relates to steeply sloped, rugged areas. Uplands in the Missouri study area are often very stony, with limited fine earth fraction—such as scree fields. Because stones are excluded in bulk density calculations The high porosity of these areas and stone content results in low bulk densities in samples.

## Bulk Density Model Performance

Adjusted R-squares for the Colorado, Minnesota, and Missouri study areas were 0.21, 0.16 and 0.19, respectively. Relative RMSE values for all three models indicate that the Colorado model had the best relative performance, with an RRMSE of 0.11, while the Minnesota and Missouri study areas had RRMSE values of 0.23 and 0.32, respectively. Model performance was poor for all three study areas. Possible explanations for this result closely mirror explanations for the poorer performing stoniness models. A linear model may have been the incorrect choice, despite attempts to identify potential nonlinear relationships prior to selection of a linear model. StepAIC reduction may have been too selective, eliminating all principal components when a less selective process might have generated results. And, finally, the predictor variables chosen may not have been sufficient to generate viable results.

Some attempts to predict or estimate bulk density, such as Sequiera, et al (2014), have used a combination of 12 pedotransfer functions, soil data from 2,680 pedons in the USDA-NRCS National Soil Survey Center database, and a random forest model to generate predictions for soil bulk density. Sequiera, et al (2014) created pedotransfer functions based on 4 properties derived from the soil horizon—texture, depth, thickness and horizon classification—while 5 properties were derived "from a horizon that could be above or below and adjacent or not adjacent to the horizon of interest" (pg. 66). These properties were bulk density, horizon classification, texture, thickness and depth (Sequeira et al. 2014). For the 12 pedotransfer functions, r-square values ranging from 0.50 – 0.71 were reported, with root mean square prediction errors (RMSPE) between 0.10 and 0.15 $g/cm^{-3}$ (Sequeira et al. 2014).

Curtis and Post (1964) used soil organic matter content to estimate the bulk density of soils in Vermont forests using soil organic matter. Curtis and Post found a strong relationship between bulk density and SOM. Furthermore, they conclude directly measuring soil bulk density in stony soils is often highly unreliable, even in best-case scenarios (Curtis and Post 1964).

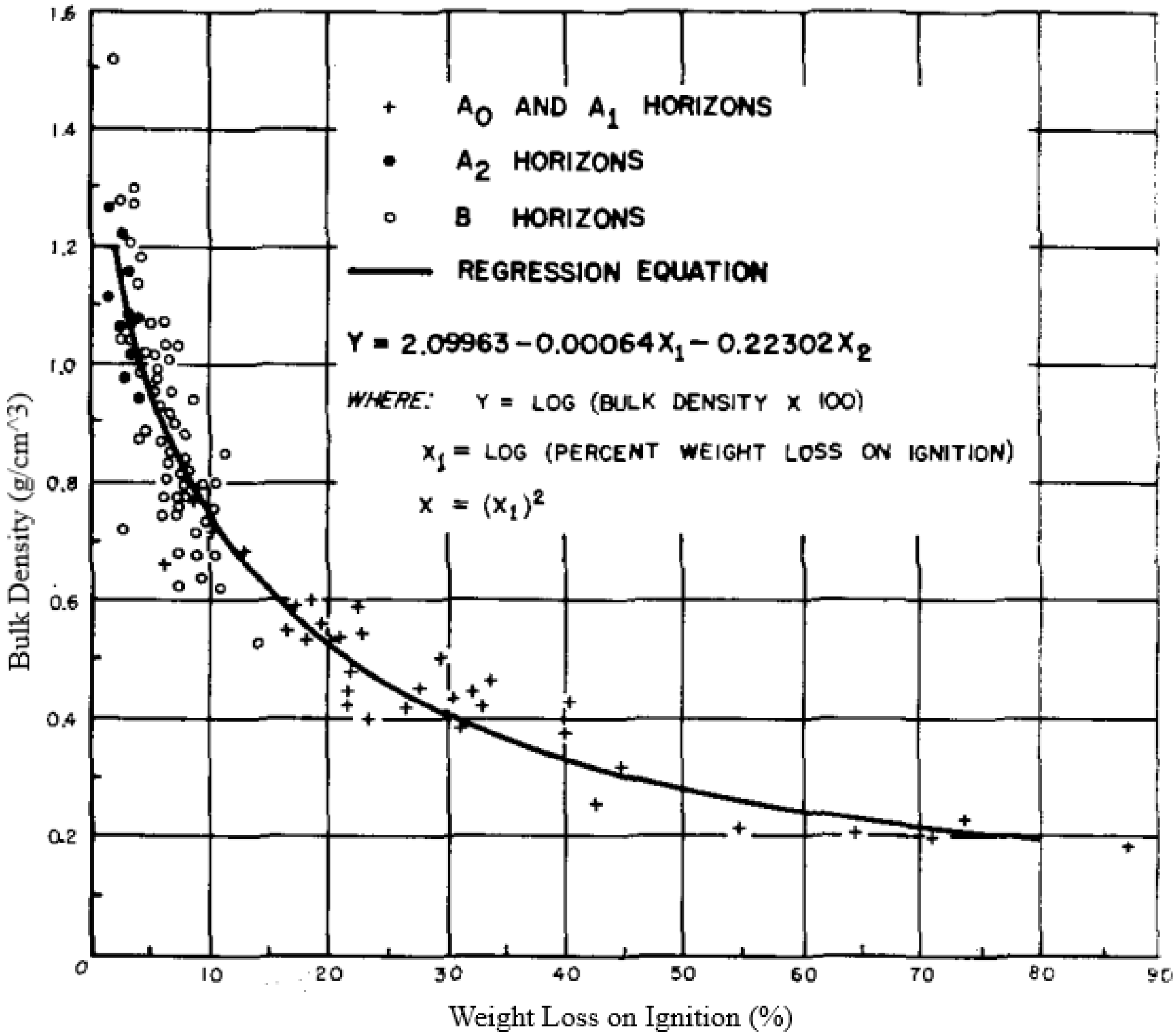


**Figure 9: Reproduction of bulk density-SOM chart from Curtis and Post (1964, pg. 286).**

## Comparison to Curtis and Post (1964) Function

The relationship between bulk density and soil organic matter (SOM) observed (Figure 10) for all three study sites mirrors the observations in Ruehlmann and Körschens (2009), whereby there is a negative relationship between soil bulk density and SOM. When compared with bulk density predictions derived from the equation in Curtis and Post (1964) for Vermont forest soils, my collected data has a correlation of 0.87, an RMSE of 0.15, and a mean error of

0.026 g/cm$^3$, indicating the predicted values from this equation were marginally higher than the observations, on average. In general, this equation fits well with the data, but noticeable differences exist. In particular, many samples have significantly lower bulk densities than predicted by the equation for low SOM samples. In many cases, these locations are from the Missouri study area, where soils on the slopes were porous, high in stone content, and low in SOM. Because stones were sieved out of my samples prior to bulk density calculation and little fine earth is present, these sampled tended towards low bulk density values. At higher SOM values, observed data was more dispersed, but also generally lower than the predictions made through the equation. This is potentially because in cases of samples with very high organic matter concentrations, large quantities of roots needed to be removed, thereby reducing the overall mass of the sample.

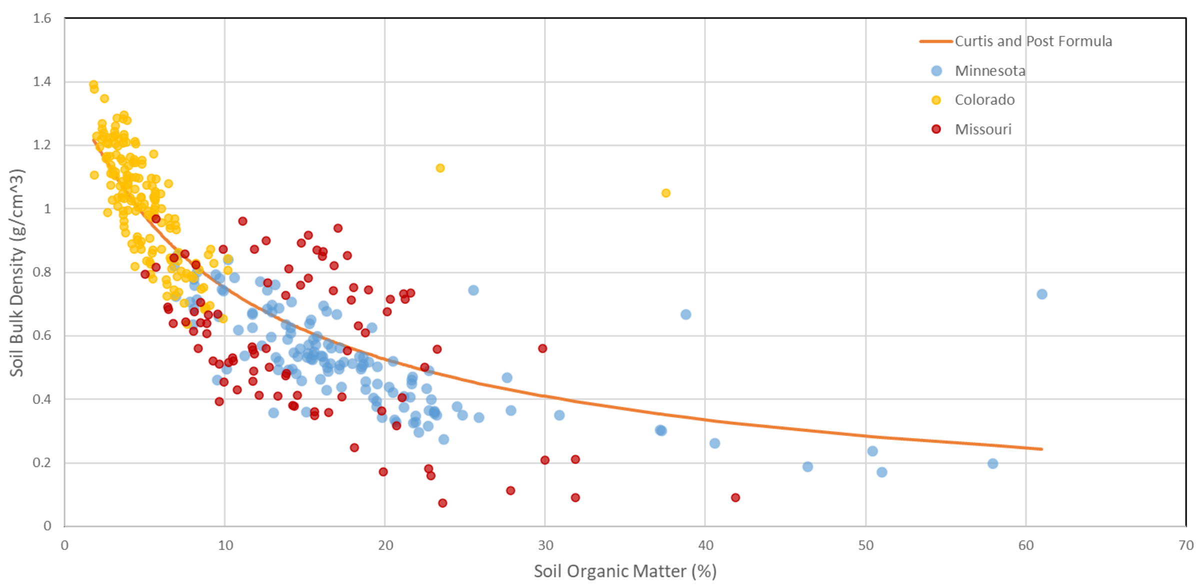


**Figure 10: Comparison of the Curtis and Post (1964) equation to my complete dataset.**

## Comparison to SSURGO

While my attempt to identify relationships between soil bulk density and stoniness was unsuccessful, other sources of soil information also struggle to provide reliable data. SSURGO (Soil Survey Staff) is a database of soil information collected and maintained by the USDA-NRCS. This database contains an array of soil information, albeit with notable limitations. The SSURGO database contains maximum and minimum possible values alongside values deemed 'representative' of a given soil body (Libohova et al. 2014, USDA-NRCS 2013) for some soil data. However, when available, these measures can be derived from three different methodologies, with little to no information provided indicating which methodology was used (Libohova et al. 2014). The highest quality method involves direct laboratory testing, such as what I have done to calculate bulk density and stoniness. However, reported SSURGO data may also be derived from field observations, both field and lab data, or even guesswork (Libohova et al. 2014). However, in spite of these concerns, Libohova, et al. (2014) find that, based on a comparison of surface SSURGO pedon-level observations and representative estimates of soil texture (sand, silt, clay), cation exchange capacity, and pH, that "no significant differences between" estimated representativeness values found in SSURGO and the data that underlies them (Libohova, et al. 2014 p.66). They conclude SSURGO estimates and measured upper and lower values are viable for use in predictive modelling and examination of uncertainty (Libohova et al. 2014).

However, SSURGO data is more complicated for soil stoniness. Rather than provide a single measure of soil stone content, to calculate stoniness from SSURGO data, one must use a series of estimates or measures of the mass of stones greater than 10 inches, the mass between 3 and 10 inches, and then a percent of the mass of matter less than 3 inches in size that passed through a 2mm sieve to determine a stoniness by mass of the total sample. However, without knowing the density of the stones or the total mass involved, a volumetric estimate of stoniness is impossible.

For the gSSURGO data available in the Missouri study area, representative oven dry bulk density listed within the study area ranges from 0.33 to 1.51 g/cm$^3$. In Minnesota, bulk density values ranging from 0.17 to 2.07 were reported. For Colorado, gSSURGO oven dry data provides a minimum of 1.4 and maximum of 1.67 g/cm$^3$ for bulk density in the study area. Both the minimum and maximum values in Colorado significantly higher than the 1.01 g/cm$^3$ average I calculated.

Table 25: gSSURGO bulk density ranges compared to my calculated bulk density average.

| Site | gSSURGO Min BD (g/cm$^3$) | gSSURGO Max BD (g/cm$^3$) | Calculated BD (g/cm$^3$) |
|---|---|---|---|
| Colorado | 1.4 | 1.67 | 1.01 |
| Minnesota | 0.17 | 2.07 | 0.52 |
| Missouri | 0.33 | 1.51 | 0.59 |

Possible explanations for this relate to the methodology used to calculate bulk density. While the exact methods—including processing, formulas, and handling of stones—are not specified in SSURGO data, my own data includes only the fine earth fraction after the removal of soil organic matter and is based on the original ring volume. If stones and/or soil organic matter are included in the SSURGO calculations, it is possible their values would skew higher than my own. Furthermore, it is not clear exactly where these samples were taken, or under what conditions. It may be that the soil was sampled outside of my study area, but the representative values derived were applied to soil bodies within it. Without additional information from the SSURGO data, it is difficult to determine the cause of disagreement between gSSURGO values and my own.

### Prediction of Other Soil Properties

While the focus of my work has been on soil bulk density and stoniness, substantial volumes of work on the modelling and prediction of other soil physical properties exists. Research into the prediction of properties related to bulk density, stoniness, and soil organic matter are a lens through which my own research can be examined—particularly in cases where spectral and/or geomorphometric data were used in the prediction process. For instance, in some soil orders, such as Aridisols, clay is one of the strongest influencers of bulk density (Heuscher et al. 2005). Attempts to predict soil texture properties often involve the use of infrared spectrum remote sensing data (Tümsavaş et al. 2018, Sawut et al. 2014). Tümsavaş, et al. (2018) collected 86 samples from a single agricultural field and used a mobile spectrometer to measure the surface spectral response of the soil within a trench. In the lab, soil samples were processed to remove roots and stones, and to ensure soil textures were mixed to ensure even in-sample distribution. Collected soil samples underwent laboratory spectrometer scans. Principal component analysis was performed, with two principal components used in a partial least squares regression model. Ultimately, very strong r-square values were found, with the cross validation set, laboratory prediction set, and on-line prediction sets generating r-squares of 0.81, 0.90, and 0.80 respectively for sand, while r-sqaures of 0.85, 0.91, and 0.82 were reported for the same data in clay, while silt correlations were not found (Tümsavaş et al. 2018).

Pinheiro, et al. (2017) collected 434 samples, including 96 soil horizons in an 80-square kilometer study area in the Geólogo Pedro De Moura region of Brazil to test the predictive capabilities of VIS-NIR spectroscopy for SOC, pH, Ca, Mg, Al, H. H+Al, P, CEC, sum of bases, Al saturation, percent of base saturation, soil texture (clay, sand, and silt), flocculation, and silt:clay ratio. After sample collection, samples were dried and sieved, followed by lab analysis of soil chemistry and texture. Much like with Tümsavaş, et al. (2018), samples were scanned with a laboratory spectrometer, though in this case, visible spectrum light was included in the analysis (Pinheiro et al. 2017). Results of their regression models indicate both clay contents and SOC were the best predicted variables, with r-squares of 0.78 and 0.71, respectively. Other variables, such as sand ($R^2$: 0.62), silt:clay ratio ($R^2$: 0.62), H ($R^2$: 0.78, but with a worse residual prediction deviation than clay or SOC), Al ($R^2$: 0.63), H+Al ($R^2$: 0.70), CEC ($R^2$: 0.68), Al saturation ($R^2$: 0.59) and percentage of base saturation ($R^2$: 0.50) were "moderately well predicted" through the models (Pinheiro, et al. 2017, pg. 10). Pinheiro, et al (2017) conlcude that diffuse reflectance spectroscopy provides substantial value in predicting soil properties for soil studies.

Ahmed and Iqbal (2014) collected 170 soil samples in a Punjab, Pakistan study area to asses the value of Landsat 5 data in predicting soil texture and organic matter content. Images were selected from months in which bare soil was most visible, and a nearest neighbor technique was applied to the image to further reduce the number of cells featuring returns from vegetation. Additionally, a filter to reduce haze was applied to the imagery. Cells still containing water or vegetation returns were removed by calculating NDVI and NDWI indexes, then extracting cells with values high enough to suggest they were water or vegetation returns. Areas identified as water or vegetation were excluded from analysis. Multivariate linear regression modelling was used to assess the predictive capabilities of the Landsat TM 5 bands. Band 4, NIR, was strongly positively correlated with soil texture—a classified variable—while thermal returns, band 6, were very negatively correlated. Soil organic matter was negatively correlated with all bands, but was most strongly so with visible sprectrum and thermal returns—a result of the dark color typically associated with organic matter (Ahmed and Iqbal 2014). The results of the linear regression modelling showed adjusted r-square values for clay, silt and SOM as 0.501, 0.720, and 0.534, respectively (Ahmed and Iqbal 2014).

In general, these efforts to predict soil properties perform better than my own attempts at prediction of bulk density and soil stoniness, even when performed with similar (i.e. LANDSAT) data on a regional scale.  In the case of Ahmed and Iqbal (2014), while a smaller explanatory dataset is used when compared to my own, a number of differences in the usage of their multispectral data proved future avenues for exploration. For one, they applied additional haze correction and the removal of water and more vegetated areas from the imagery, thereby ensuring the returns were predominantly of the surface. In my case, no additional preprocessing was used. Had such measures been taken, it is possible the multispectral data would have been a stronger contributor to the models in Missouri or Colorado, but far too much of the Minnesota study area was covered in vegetation for vegetation removal to have been a good strategy. The second key difference is Ahmed and Iqbal's (2014) use of multispectral indexes—specifically NDVI and NDWI—in conjunction with the original spectral band returns. Such indexes may allow for more robust capturing of the vegetative health and the amount of water present in the study area, potentially improving model performance.

The study area used is described by the authors as a flat, "semi-arid subtropical continental" region, with "soil parent material…mainly [consisting] of mixed calcerious aluvium (e.g. calcareous sandstone, granites, shale and clays, schists, gneisses and slates) in the Hamalayas" (Ahmed and Iqbal 2014, p.560). Climatically, this region is most similar to the Colorado study area, where flat, semi-arid landscapes dominate both. In terms of parent material, similarities with Colorado again seem to arise. It is possible, then, such an approach could prove useful in the Colorado study area. With respect to the other two study areas, major contrasts can be made in the CLORPT function. Both are more rugged, both have substantially higher annual rainfall, one has glacial till as a major source of parent material, while the other has parent material provided from upslope. In both, vegetation is likely to be more prominent, such that exclusion of vegetated areas would significantly curtail the size of the study areas.

In the case of both Pinheiro, et al. (2017) and Tümsavaş, et al. (2018), it is clear that spectroscopy may represent an alternative means of studying the relationship between multispectral returns and soil properties. In both, moderate-high strength r-squares were found between selected soil physical and chemical properties. However, significant limitations to the widespread implementation of these procedures can be identified. Tümsavaş, et al. (2018) created trenches in a roughly 10 hectacre field and drove a tractor carring a spectrometer over them to collect soil spectral data. My focus is on land too rugged for conventional agricultural techniques. Not only would this method be impossible in such circumstances, it requires specialized equipment, is labor intensive, and potentially destructive. These drawbacks make their methods infeasible for widespread deployment. Pinheiro, et al. (2017) examined a much larger study area (80 $km^2$) and sampled multiple horizons at each location. Multispectral data for the samples were collected only in the lab—no satellite data was used. Unlike with Tümsavaş, et al. (2018), no special equipment or particularly laborious proceedures were used in the field (Pinheiro et al. 2017). As such, their methodology is likely more feasible for rough, steep, or stony terrain.

## Conclusions

In the case of the stoniness models, reported r-square values were very low for the Minnesota and Missouri study areas—0.02 and 0.05, respectively. In these cases, the stoniness model was not capable of generating strong predictions given the available data. A limited number of sample sites could be a contributing factor, while heavy vegetation served to limit the value of the multispectral data by obstructing returns from the soil itself. In the case of the Colorado study area, a moderate r-square of 0.56 was achieved, though RMSE was high, at 0.43. Improvements to r-square may pertain to reduced variation in stoniness, subdued topography, and limited vegetation.

The landscape characteristics with the strongest association to stoniness differed between sites. Of those that could be identified in Colorado, wet areas, and rugged slopes near channels had the strongest negative correlation to stoniness, PC1, wet, flat areas away from channels, could be explained with field observations, while the other two components could not. For Minnesota, only one PC had a correlation stronger than +/-0.2—flat, near-channel areas. These locations likely include wetlands and other low energy environments, in which lower stoniness was observed in the field. For the Missouri stoniness model, the most important landscape features influencing stoniness appeared to be flat areas. Flat areas near ridges were associated with higher stoniness, while flat, wet areas correlated to lower stoniness.

For bulk density, adjusted r-squares were 0.16, 0.19, and 0.21 for the Minnesota, Missouri, and Colorado study areas, respectively. RMSE values were 0.11 for Colorado, 0.12 for Minnesota, and 0.19 for Missouri. R-square values suggest a weak relationship between the geomorphometric variables, multispectral data, and bulk density for all three study areas.

Relative RMSE values confirm the Missouri study area had the highest error, with an RRMSE of 0.32, compared to 0.23 for Minnesota and 0.11 for Colorado.

As with the stoniness models, topographic characteristics could be identified among the PCs for each study area. Topographic characteristics for the Colorado study area were gentle hills away from channels and locally wet areas. Both were associated with higher bulk density, whereby correlations of 0.27 and 0.37, respectively, were found. PC5, hills away from channels, could be explained through a lens of field experience, but PC9, the locally wet areas, could not. One component in Minnesota, PC1, had a moderate negative correlation of -0.39 and was associated with wet, flat areas close to channels. This association matched field observations of the study area. Areas fitting the characteristics of PC1, such as wetlands, frequently had higher quantities of organic material, contributing to a lower bulk density. Of the three components from the Missouri study area, the two that could be identified had weak-moderate negative correlations with bulk density—flat uplands near ridges and steep, rugged terrain. This is a direct consequence of the high stoniness and small fine earth fraction found there. In general, performance for the bulk density and stoniness models was poor, with only the Colorado stoniness model serving as an exception. The Minnesota and Missouri stoniness model r-squares demonstrate no relationship could be established between the suite of variables and stoniness at either study site. For bulk density, weak r-squares were recorded for all three study areas, though relative RMSE values indicate the Colorado study area performed the best in this respect.

The need for further research into the relationship between soil stoniness, bulk density, and other physical properties remains strong. Despite the use of a wide array of geomorphometric variables and multispectral data, resulting correlations provided minimally useful insights. Such avenues could seek to explore additional geomorphometric variables, and the inclusion of multispectral indexes, rather than merely multispectral bands. While I sampled based on representative curvature and TWI, it is possible an alternative basis for sampling would have been more effective at each study area. Additional data processing techniques and the inclusion of indexes, such as with Ahmed and Iqbal (2014), may have improved results. Furthermore, linear models may not have been the best choice, despite efforts to identify nonlinear relationships in the data. It is possible that alternatives, such as decision trees, kriging, or random forest may have been more suitable. Ultimately, while the use of multiple scale geomorphometric variables remains an exciting opportunity to enhance predictive capabilities for select soil physical properties, much work remains to be done to generate successful predictive models for bulk density and stoniness.

References


Ahmed, Z. & J. Iqbal (2014) Evaluation of Landsat TM5 Multispectral Data for Automated Mapping of Surface Soil Texture and Organic Matter in GIS. *European Journal of Remote Sensing,* 47**,** 557-573.

Al-Shammary, A. A. G., A. Z. Kouzani, A. Kaynak, S. Y. Khoo, M. Norton & W. Gates (2018) Soil Bulk Density Estimation Methods: A Review. *Pedosphere,* 28**,** 581-596.

Alexander, E. (1981) Volume estimates of coarse fragments in soils: A combination of visual and weighing procedures. *Journal of Soil and Water Conservation,* 36**,** 360-361.

Alexandratos, N. & J. Bruinsma. 2012. World agriculture towards 2030/2050: the 2012 revision. In *ESA Working Papers 12-03*.

Badgujar, C., D. Flippo & S. Welch (2022a) Artificial neural network to predict traction performance of autonomous ground vehicle on a sloped soil bin and uncertainty analysis. *Computers and Electronics in Agriculture,* 196**,** 106867.

Badgujar, C. M., D. Flippo, E. Brokesh & S. Welch (2022b) Experimental Investigation on Traction, Mobility, and Energy Usage of a Tracked Autonomous Ground Vehicle on a Sloped Soil Bin. *Journal of Agricultural Safety and Health,* 65**,** 835-847.

Bauer, T., P. Strauss & E. Murer (2014) A photogrammetric method for calculating soil bulk density. *Journal of Plant Nutrition and Soil Science,* 177**,** 496-499.

Beckett, S. H. (1928) The Use of Highly Viscous Fluids In The Determination of Volume-Weight of Soils. *Soil Science,* 25**,** 481-484.

Beven, K. J. & M. J. Kirkby (1979) A physically based, variable contributing area model of basin hydrology / Un modèle à base physique de zone d'appel variable de l'hydrologie du bassin versant. *Hydrological Sciences Bulletin,* 24**,** 43-69.

Bivand, R., T. Keitt & B. Rowlingson. 2019. rgdal: Bindings for the 'Geospatial' Data Abstraction Library. R package version 1.4-8.

Blake, G. & K. Hartge. 1986. Bulk density. In *Methods of soil analysis: Part 1 Physical and mineralogical methods,* ed. A. Klute, 363-375. Madison, Wisconsin: American Society of Agronomy.

Blake, G. R. 1965. Bulk Density. In *Methods of Soil Analysis: Part 1,* ed. C. A. Black, 383-390. Madison, WI: American Society of Agronomy.

Brenning, A., D. Bangs & M. Becker. 2018. RSAGA: SAGA Geoprocessing and Terrain Analysis. R Package version 1.3.0.

Brunsdon, C., S. Fotheringham & M. Charlton (1998) Geographically Weighted Regression. *Journal of the Royal Statistical Society: Series D (The Statistician),* 47**,** 431-443.

Burrough, P. A. & R. A. McDonnell. 1998. Spatial Analysis Using Continuous Fields. In *Principles of Geographical Information Systems,* 183-236. Oxford, United Kingdom: Oxford University Press.

Campbell, D. 1994. Determination and use of soil bulk density in relation to soil compaction. In *Developments in Agricultural Engineering,* 113-139. Elsevier.

Carré, F., A. B. McBratney & B. Minasny (2007) Estimation and potential improvement of the quality of legacy soil samples for digital soil mapping. *Geoderma,* 141**,** 1-14.

Carrick, S., D. Palmer, T. Webb, J. Scott & L. Lilburne. 2013. Stony soils are a major challenge for nutrient management under irrigation development. In *Accurate and efficient use of nutrients on farms,* 1-8.

Chaudhari, P. R., D. V. Ahire, V. D. Ahire, M. Chkravarty & S. Maity (2013) Soil bulk density as related to soil texture, organic matter content and available total nutrients of Coimbatore soil. *International Journal of Scientific and Research Publications,* 3**,** 1-8.

Cressie, N. (1990) The origins of kriging. *Mathematical Geology,* 22**,** 239-252.

Curtis, R. O. & B. W. Post (1964) Estimating Bulk Density from Organic-Matter Content in Some Vermont Forest Soils. *Soil Science Society of America Journal,* 28**,** 285-286.

Dam, R. F., B. B. Mehdi, M. S. E. Burgess, C. A. Madramootoo, G. R. Mehuys & I. R. Callum (2005) Soil bulk density and crop yield under eleven consecutive years of corn with different tillage and residue practices in a sandy loam soil in central Canada. *Soil and Tillage Research,* 84**,** 41-53.

Deans, J. & R. Milne (1978) An electrical recording soil moisture tensiometer. *Plant and Soil,* 50**,** 509-513.

Dobos, E., L. Montanarella, T. Nègre & E. Micheli (2001) A regional scale soil mapping approach using integrated AVHRR and DEM data. *International Journal of Applied Earth Observation and Geoinformation,* 3**,** 30-42.

Don, A., J. Schumacher, M. Scherer-Lorenzen, T. Scholten & E.-D. Schulze (2007) Spatial and vertical variation of soil carbon at two grassland sites — Implications for measuring soil carbon stocks. *Geoderma,* 141**,** 272-282.

Eldeiry, A. A. & L. A. Garcia (2008) Detecting Soil Salinity in Alfalfa Fields using Spatial Modeling and Remote Sensing. 72**,** 201.

Erbach, D. C. (1987) Measurement of Soil Bulk Density and Moisture. *Transactions of the ASAE,* 30**,** 922-0931.

Flack, V. F. & P. C. Chang (1987) Frequency of selecting noise variables in subset regression analysis: a simulation study. *The American Statistician,* 41**,** 84-86.

Foley, J. A., N. Ramankutty, K. A. Brauman, E. S. Cassidy, J. S. Gerber, M. Johnston, N. D. Mueller, C. O'Connell, D. K. Ray & P. C. West (2011) Solutions for a cultivated planet. *Nature,* 478**,** 337-342.

Forkuor, G., O. K. L. Hounkpatin, G. Welp & M. Thiel (2017) High Resolution Mapping of Soil Properties Using Remote Sensing Variables in South-Western Burkina Faso: A Comparison of Machine Learning and Multiple Linear Regression Models. *PLOS ONE,* 12**,** e0170478.

Hammer, B. & M. Frasco. 2018. Metrics: Evaluation Metrics for Machine Learning.

Häring, T., E. Dietz, S. Osenstetter, T. Koschitzki & B. Schröder (2012) Spatial disaggregation of complex soil map units: A decision-tree based approach in Bavarian forest soils. 185-186**,** 37-47.

Hartfield, K. A., K. I. Landau & W. J. D. V. Leeuwen (2011) Fusion of High Resolution Aerial Multispectral and LiDAR Data: Land Cover in the Context of Urban Mosquito Habitat. *Remote Sensing,* 3**,** 2364-2383.

Hebbali, A. 2020. olsrr: Tools for Building OLS Regression Models. CRAN.

Heuscher, S. A., C. C. Brandt & P. M. Jardine (2005) Using Soil Physical and Chemical Properties to Estimate Bulk Density. *Soil Science Society of America Journal,* 69**,** 51-56.

Hijmans, R. J., J. van Etten, M. Sumner, J. Cheng, D. Baston, A. Bevan, R. Bivand, L. Busetto, M. Canty, B. Fasoli, D. Forrest, A. Ghosh, D. Golicher, J. Gray, J. A. Greenberg, P. Hiemstra, K. Hingee, A. Ilich, Institute for Mathematics Applied Geosciences, C. Karney, M. Mattiuzzi, S. Mosher, B. Naimi, J. Nowosad, E. Pebesma, O. P. Lamigueiro,

E. B. Racine, B. Rowlingson, A. Shortridge, B. Venables & R. Wueest. 2020. raster: Geographic Data Analysis and Modelling. In *Package 'raster'*.

Hoogsteen, M. J. J., E. A. Lantinga, E. J. Bakker, J. C. J. Groot & P. A. Tittonell (2015) Estimating soil organic carbon through loss on ignition: effects of ignition conditions and structural water loss. *European Journal of Soil Science,* 66**,** 320-328.

Hovde Liland, K., B.-H. Mevik, R. Wehrens & P. Hiemstra. 2021. pls: Partial Least Squares and Principal Component Regression.

Hudson, B. D. (1992) The Soil Survey as Paradigm-based Science. *Soil Science Society of America Journal,* 56**,** 836-841.

Komista, L. & F. Novomestky. 2015. moments: Moments, cumulants, skewness, kurtosis, and related tests.

Krige, D. 1976. A review of the development of geostatistics in South Africa. In *Advanced geostatistics in the mining industry,* 279-293. Springer.

Krige, D. G. (1951) A statistical approach to some basic mine valuation problems on the Witwatersrand. *Journal of the Southern African Institute of Mining and Metallurgy,* 52**,** 119-139.

Lagacherie, P. & A. B. McBratney. 2006. Chapter 1: Spatial Soil Information Systems and Spatial Soil Inference Systems: Perspectives for Digital Soil Mapping. In *Developments in Soil Science,* eds. P. Lagacherie, A. B. McBratney & M. Voltz, 3-22. Elsevier.

Lam, N. S.-N. (1983) Spatial interpolation methods: a review. *The American Cartographer,* 10**,** 129-150.

Lambin, E. F. 2001. Remote Sensing and Geographic Information Systems Analysis. In *International Encyclopedia of the Social & Behavioral Sciences,* eds. N. J. Smelser & P. B. Baltes, 13150-13155. Oxford: Pergamon.

Lane, P. W. (2002) Generalized linear models in soil science. *European Journal of Soil Science,* 53**,** 241-251.

Lesch, S. M., D. J. Strauss & J. D. Rhoades (1995) Spatial prediction of soil salinity using electromagnetic induction techniques: 1. Statistical prediction models: A comparison of multiple linear regression and cokriging. *Water Resources Research,* 31**,** 373-386.

Libohova, Z., S. Wills & N. Odgers. 2014. Legacy data quality and uncertainty estimation for United States GlobalSoilMap products. In *GlobalSoilMap: Basis of the Global Spatial Soil Information System,* ed. N. M. Dominique Arrouays, Jon Hempel, Anne Richer de Forges, Alex B. McBratney, 63-68. CRC Press.

Logsdon, S. D. & D. L. Karlen (2004) Bulk density as a soil quality indicator during conversion to no-tillage. *Soil and Tillage Research,* 78**,** 143-149.

Loh, W.-L. (1996) On Latin hypercube sampling. *The Annals of Statistics,* 24**,** 2058-2080.

McBratney, A. B., M. L. Mendonça Santos & B. Minasny (2003) On digital soil mapping. *Geoderma,* 117**,** 3-52.

McBratney, A. B. & M. J. Pringle (1999) Estimating Average and Proportional Variograms of Soil Properties and Their Potential Use in Precision Agriculture. *Precision Agriculture,* 1**,** 125-152.

McKenzie, N. & M. Austin (1993) A quantitative Australian approach to medium and small scale surveys based on soil stratigraphy and environmental correlation. *Geoderma,* 57**,** 329-355.

McLintock, T. F. (1959) A Method for Obtaining Soil-Sample Volumes in Stony Soils. *Journal of Forestry,* 57**,** 832-834.

Miles, J. 2005. R-Squared, Adjusted R-Squared. In *Encyclopedia of Statistics in Behavioral Science*.
Miller, B. A., S. Koszinski, M. Wehrhan & M. Sommer (2015) Impact of multi-scale predictor selection for modeling soil properties. *Geoderma,* 239-240**,** 97-106.
Minasny, B., P. Finke, U. Stockmann, T. Vanwalleghem & A. B. McBratney (2015) Resolving the integral connection between pedogenesis and landscape evolution. *Earth-Science Reviews,* 150**,** 102-120.
Minasny, B., A. McBratney, N. McKenzie & M. Grundy (2009) Predicting soil properties using pedotransfer functions and environmental correlation.
Minnesota Department of Natural Resources. 2003. Finland State Forest Trail Map. 1-2.
Minnesota Geological Survey, Lusardi, B.A. (2017) Minnesota at a Glance: Quaternary Glacial Geology.
Missouri Department of Natural Resources. 2020. Roaring River State Park Data Sheet. Missouri Department of Natural Resources.
Mora-Vallejo, A., L. Claessens, J. Stoorvogel & G. B. Heuvelink (2008) Small scale digital soil mapping in Southeastern Kenya. *Catena,* 76**,** 44-53.
Myles, A. J., R. N. Feudale, Y. Liu, N. A. Woody & S. D. Brown (2004) An introduction to decision tree modeling. *Journal of Chemometrics,* 18**,** 275-285.
Nelder, J. A. & R. W. Wedderburn (1972) Generalized linear models. *Journal of the Royal Statistical Society: Series A (General),* 135**,** 370-384.
Omran, E.-S. E. (2012) Improving the Prediction Accuracy of Soil Mapping through Geostatistics. 03**,** 574-590.
Pebesma, E. J. & R. S. Bivand (2005) Classes and methods for spatial data in R. *R News,* 5.
Pebsama, E. (2018) Simple Features for R: Standardized Support for Spatial Vector Data. *The R Journal,* 10**,** 439 - 446.
Pinheiro, É. F., M. B. Ceddia, C. M. Clingensmith, S. Grunwald & G. M. Vasques (2017) Prediction of soil physical and chemical properties by visible and near-infrared diffuse reflectance spectroscopy in the central Amazon. *Remote Sensing,* 9**,** 293.
Poeplau, C., C. Vos & A. Don (2017) Soil organic carbon stocks are systematically overestimated by misuse of the parameters bulk density and rock fragment content. *SOIL,* 3**,** 61-66.
Popova, L., D. Van Dusschoten, K. A. Nagel, F. Fiorani & B. Mazzolai (2016) Plant root tortuosity: an indicator of root path formation in soil with different composition and density. *Annals of Botany,* 118**,** 685-698.
PRISM Climate Group at Oregon State University. 2012. All 30-year normals, 4km resolution.
Ray, D. K., N. Ramankutty, N. D. Mueller, P. C. West & J. A. Foley (2012) Recent patterns of crop yield growth and stagnation. *Nature Communications,* 3**,** 1293.
Refaeilzadeh, P., L. Tang & H. Liu. 2009. Cross-Validation. 532-538. Springer US.
Reinhart, K. (1961) The Problem of Stones in Soil-Moisture Measurement 1. *Soil Science Society of America Journal,* 25**,** 268-270.
Riley, S. J., S. D. DeGloria & R. Elliot (1999) Index that quantifies topographic heterogeneity. *Intermountain Journal of Sciences,* 5**,** 23-27.
Roudier, P. 2011. clhs: a R package for conditioned Latin hypercube sampling.
Różycka, M., P. Migoń & A. Michniewicz (2017) Topographic Wetness Index and Terrain Ruggedness Index in geomorphic characterisation of landslide terrains, on examples from

the Sudetes, SW Poland. *Zeitschrift für geomorphologie, Supplementary issues,* 61**,** 61-80.
Ruehlmann, J. & M. Körschens (2009) Calculating the Effect of Soil Organic Matter Concentration on Soil Bulk Density. *Soil Science Society of America Journal,* 73**,** 876-885.
Samouëlian, A., I. Cousin, A. Tabbagh, A. Bruand & G. Richard (2005) Electrical resistivity survey in soil science: a review. *Soil and Tillage Research,* 83**,** 173-193.
Sanchez, P. A., S. Ahamed, F. Carré, A. E. Hartemink, J. Hempel, J. Huising, P. Lagacherie, A. B. McBratney, N. J. McKenzie, M. d. L. Mendonça-Santos, B. Minasny, L. Montanarella, P. Okoth, C. A. Palm, J. D. Sachs, K. D. Shepherd, T.-G. Vågen, B. Vanlauwe, M. G. Walsh, L. A. Winowiecki & G.-L. Zhang (2009) Digital Soil Map of the World. *Science,* 325**,** 680.
Sawut, M., A. Ghulam, T. Tiyip, Y.-j. Zhang, J.-l. Ding, F. Zhang & M. Maimaitiyiming (2014) Estimating soil sand content using thermal infrared spectra in arid lands. *International Journal of Applied Earth Observation and Geoinformation,* 33**,** 203-210.
Schoeneberger, P. J., D. A. Wysocki, E. C. Benham & S. S. Staff. 2012. *Field book for describing and sampling soils*. Washington, D.C.: Government Printing Office.
Sequeira, C. H., S. A. Wills, C. A. Seybold & L. T. West (2014) Predicting soil bulk density for incomplete databases. *Geoderma,* 213**,** 64-73.
Soil Survey Staff, N. R. C. S., United States Department of Agriculture. Soil Survey Geographic (SSURGO) Database.
Sørensen, R., U. Zinko & J. Seibert (2006) On the calculation of the topographic wetness index: evaluation of different methods based on field observations. *Hydrology and Earth System Sciences,* 10**,** 101-112.
Stoorvogel, J. J., M. Bakkenes, A. J. A. M. Temme, N. H. Batjes & B. J. E. Brink (2017) S-World: A Global Soil Map for Environmental Modelling. *Land Degradation & Development,* 28**,** 22-33.
Sykes, A. O. (1993) An introduction to regression analysis. *Coase-Sandor Institute for Law & Economics - Working Paper,* 20**,** 1-33.
Taghizadeh-Mehrjardi, R., F. Sarmadian, B. Minasny, J. Triantafilis & M. Omid (2014) Digital mapping of soil classes using decision tree and auxiliary data in the Ardakan region, Iran. *Arid Land Research and Management,* 28**,** 147-168.
Temme, A. J., J. M. Schoorl & W. M. van der Meij (2022) New geomorphometric variables for non-continuous hillslopes – Assessing the value for digital soil mapping. *Geoderma,* 418**,** 115848.
Tetegan, M., C. Pasquier, A. Besson, B. Nicoullaud, A. Bouthier, H. Bourennane, C. Desbourdes, D. King & I. Cousin (2012) Field-scale estimation of the volume percentage of rock fragments in stony soils by electrical resistivity. *Catena,* 92**,** 67-74.
Tümsavaş, Z., Y. Tekin, Y. Ulusoy & A. M. Mouazen (2018) Prediction and mapping of soil clay and sand contents using visible and near-infrared spectroscopy. *Biosystems Engineering,* 177**,** 90-100.
United States Forest Service. Pawnee National Grassland.
US Geological Survey. 2019-2022. EarthExplorer LANDSAT Level 2 Collection.
---. 2021-2022. 3DEPElevationIndex (MapServer). ed. U. G. Survey.
USDA-NRCS. 2013. *National Soil Survey Handbook*. United States Department of Agriculture-Natural Resources Conservation Service.

USDA-NRCS Soil Science Division Staff. 2017. *Soil survey manual*. Washington, D.C.: Government Printing Office.

USDA-NRCS Soil Survey Staff. Soil Survey Geographic (SSURGO) Database.

USDA NCRS Soil Survey Staff. Web Soil Survey.

Vanguelova, E. I., E. Bonifacio, B. De Vos, M. R. Hoosbeek, T. W. Berger, L. Vesterdal, K. Armolaitis, L. Celi, L. Dinca, O. J. Kjønaas, P. Pavlenda, J. Pumpanen, Ü. Püttsepp, B. Reidy, P. Simončič, B. Tobin & M. Zhiyanski (2016) Sources of errors and uncertainties in the assessment of forest soil carbon stocks at different scales—review and recommendations. *Environmental Monitoring and Assessment,* 188.

Venables, W. N. & B. D. Ripley. 2002. *Modern Applied Statistics with S*. New York: Springer.

Viana, F. A. C. (2016) A Tutorial on Latin Hypercube Design of Experiments. *Quality and Reliability Engineering International,* 32**,** 1975-1985.

Vincent, K. R. & O. A. Chadwick (1994) Synthesizing Bulk Density for Soils with Abundant Rock Fragments. *Soil Science Society of America Journal,* 58**,** 455-464.

Wang, W. & Y. Lu. 2018. Analysis of the mean absolute error (MAE) and the root mean square error (RMSE) in assessing rounding model. In *IOP conference series: materials science and engineering*, 012049. IOP Publishing.

Wayne, W. J., Aber, J. S., Agard, S. S., Bergantino, R. N., Bluemle, J. P., Coates, D. A., Cooley, M. E., Madole, R. F., Martin, J. E., Mears, B., Jr., Morrison, R. B., Sutherland, W. M. 1991. Quaternary geology ofthe Northern Great Plains. In *Quaternary nonglacial geology; Conterminous U.S.: Boulder, Colorado,* ed. R. B. Morrison. Geological Society of America.

Wickham, H. 2016. *ggplot2: Elegant Graphics for Data Analysis*. Verlag, New York: Springer.

Wickham, H., M. Averick, J. Bryan, W. Chang, L. McGowan, R. François, G. Grolemund, A. Hayes, L. Henry, J. Hester, M. Kuhn, T. Pedersen, E. Miller, S. Bache, K. Müller, J. Ooms, D. Robinson, D. Seidel, V. Spinu, K. Takahashi, D. Vaughan, C. Wilke, K. Woo & H. Yutani (2019) Welcome to the Tidyverse. *Journal of Open Source Software,* 4**,** 1686.

Wickham, H., R. François, L. Henry & K. Müller. 2020. dplyr: A Grammar of Data Manipulation. .

Wirth, C., E. Schulze, G. Schwalbe, S. Tomczyk, G. Weber, E. Weller, H. Böttcher, J. Schumacher & J. Vetter (2004) Dynamik der Kohlenstoffvorräte in den Wäldern Thüringens. *Abschlussbericht zur,* 1.

Xu, B. & P. Gong (2007) Land-use/Land-cover Classification with Multispectral and Hyperspectral EO-1 Data. *Photogrammetric Engineering & Remote Sensing,* 73**,** 955-965.

Zhang, Z. (2016) Variable selection with stepwise and best subset approaches. *Annals of Translational Medicine,* 4**,** 136-136.